FORSCHUNGSZENTRUM
ROSSENDORF e.V.

FZR

Archiv-Ex.:

FZR-83
April 1995

E. Persson

Threshold phenomena in an open quantum mechanical system

Forschungszentrum Rossendorf e.V.
Postfach 51 01 19 · D-01314 Dresden
Bundesrepublik Deutschland

Telefon (0351) 591 3281
Telefax (0351) 591 3700
E-Mail persson@fz-rossendorf.de

THRESHOLD PHENOMENA IN AN OPEN QUANTUM MECHANICAL SYSTEM

EMIL PERSSON

April 9, 1995

Abstract

The aim of this work is to investigate threshold phenomena in the nuclear structure caused by the coupling to the continuum of decay channels using the continuum shell model. The model is outlined and some relevant results are stated. It describes an open quantum mechanical system, the effective hamiltonian of which has complex eigenvalues, giving the widths and energies of the states.

The first series of calculations are performed to investigate the properties of the eigenvalue picture close to the elastic neutron threshold as a function of a parameter determining the coupling strength to the continuum. The main results are the following: States with energies below the threshold (called negative states) can trap resonant states. An analytical reason for this fact is stated. The negative states can directly influence the cross section.

In the second series of calculations the expansion coefficients of the open states in relation to the states of the shell model are investigated. The results help in the interpretation of the real and imaginary parts of the energy dependent eigenvalues of the effective hamiltonian. Broad width of a state corresponds not only to short lifetime, but is also connected with similarity between the wavefunction of the state and a decay channel.

Contents

Chapter 1

INTRODUCTION

Selforganization is observed in different many particle systems. This topic concerns mainly the question how order spontaneously can occur in a non-ordered system. The clearest examples of selforganization exist in biology. Evolution theory and regulation mechanisms in living beings and echosystems are splendid examples, of that order spontaneously can occur in nature without human interference. In chemistry a few examples are chemical watches and certain reactions where spatio-temporal patterns can occur. Typical for all selforganizating processes is the fast growth of certain fluctuations at the expense of other ones. Stabilisation occurs when the fluctuation can dominate a large region and 'enslave' the other possible fluctuations (trapping). The system can remain stable until a sufficiently large fluctuation destroys the stability.

In physics the concept of selforganization is connected with a certain extra challenge, because at first sight it seems incompatible with the laws of thermodynamics[1]. One has to consider the system and its environment as a whole in order to overcome this problem. Selforganization in quantum systems is investigated up to now in a few cases only. Mostly the behaviour of the system is described by means of rate equations [2][3]. A full quantum mechanical description was performed first by Rotter and co-workers for the nuclei [4][5]. By using the continuum shell model the nucleus is described as an open quantum mechanical system. In [6] and [7] it has been shown that the redistribution in the nuclear system that occurs at a critical value of the level density shows accordance with the rules formulated by Haken [3] for selforganization. Two different timescales are formed at high level density corresponding to short- and long-lived resonant states. This is the so-called trapping effect in resonance reactions, corresponding to the slaving principle, which was formulated for the laser [3]. In both cases the number of relevant degrees of freedom is reduced by the redistribution taking place in the system under critical conditions. In [8] the formation of structures in space and time is shown to appear in the nuclear system due to the trapping effect. This is in qualitative analogy with the formation of structures formulated by Prigogine [1].

The neutron resonances analysed by Bohigas et al [9] are shown to fulfill the statistical laws for quantum chaos. It has been shown that the trapped states (which are long-lived) also obey these statistical laws [10]. Thus the neutron resonances are suggested to correspond to the trapped states [5]. The neutron resonances are observed in the very neighbourhood of the elastic neutron threshold. Their widths and energy distances are

in the order of keV or even eV, which should be compared with the energy scale MeV typical for nuclei. However, up to now the trapping effect in nuclei is investigated only at energies far from thresholds[4-8, 10-15]. To see if the suggestion made above could be realistic, it therfore is necessary to investigate the trapping effect near to the elastic threshold.

The aim of this work is to investigate the trapping effect on the basis of the continuum shell model at energies close to the elastic threshold. In chapter 2, the model, allowing for the description of the open quantum mechanical system, is outlined and in chapter 3 some characteristic results are summarized. The numerical results for an ensemble close to the elastic threshold are shown in chapter 4 and discussed in chapter 5. As only neutron scattering is considered, the consideration of negative states gives rise to an intricate theoretical question. The neutrons can only have positive kinetic energy, and thus the negative states do not appear as resonances in the cross section. They certainly have no width and can not decay. Nevertheless it is shown that they can influence the states at positive energies. It would therefore be desirable if one could describe the negative states in a way independent of decay times. For that purpose the expansion coefficients of the states coupled to the continuum of decay channels with respect to the closed system states are investigated in chapter 6. A summary of the obtained results is given in chapter 7.

Chapter 2

DESCRIPTION OF THE MODEL

The aim of the continum shell model is to describe the nucleus as an open quantum mechanical system, i.e nuclear structure and nuclear reactions are treated in an unified manner. The nucleus is described by a direct numerical solution of the Schrödinger equation of the many particle system. Nucleons are assumed to move independently in a Woods-Saxon potential and the residual interaction between the nucleons are taken into accout by a two body delta interaction with spin and isospin exchange. The model is described in [5].

2.1 Closed system consideration

2.1.1 Single particle solutions

The first step is to describe the closed system as a system of many particles moving independently in a central potential,

$$H^0 = \sum_{i=1}^{A} h^0(i) \; ; \; h^0(i) = t(i) + V^0(i) \; . \tag{2.1}$$

Here V^0 is the Woods-Saxon potential, which is a standard phenomenological parametrization of the nuclear force inside the nucleus. The main features of this potential are that it has a finite depth and that it is weakly state dependent.

The potential is spherical symmetric, so we can separate the variables. The single-particle hamiltonian is

$$h_{\tau lj} = \frac{\hbar^2}{2m}\left[-\frac{d^2}{dr^2} + \frac{l(l+1)}{r^2}\right] + V_{\tau lj}(r) \; . \tag{2.2}$$

First we define

$$Y_{ljm}(\Omega) = \sum_{r\sigma} C Y_{lm}(\Omega) X_{s\sigma} \tag{2.3}$$

where C are the Clebsch-Gordan coefficients, Y_{lm} the spherical harmonics and X the spin matrix.

The single particle wavefunctions are

$$\varphi_{e\tau lj} = i^l Y_{ljm}(\Omega) X_{t\tau} \frac{1}{r} U_{e\tau lj}(r) \ . \tag{2.4}$$

Here $X_{t\tau}$ is the isospin matrix and U the radial function which can be obtained by solving 2.2. We get bound and unbound radial solutions, φ_n and φ_ε. The n and ε denote the principal quantum number of a discrete state and the energy of an unbound state respectively.

2.1.2 Many particle states

The basic many particle states (called Slater determinants) are constructed choosing a proper configuration space out of the single particle wavefunctions. In doing so we consider a certain number of holes below the fermi surface and a certain number of particles above it,

$$\mid \varphi_i^{sl}\rangle = \mathcal{A}\{\varphi_{\alpha i1} ... \varphi_{\alpha iA}\} \ . \tag{2.5}$$

Here $\mathcal{A}$ is the antisymmetrised product operator due to the Pauli principle and the indistinguishability of the particles. α_i denotes the quantum numbers for a particulary state used in the Slater determinant.

The Slater determinants are by construction solutions of H^0:

$$H^0 \mid \varphi_i^{sl}\rangle = E_i^0 \mid \varphi_i^{sl}\rangle \ ; \ E_i^0 = \sum \varepsilon_n \tag{2.6}$$

Note that the energies of the many particle states can lie above particle decay thresholds although they are formed out of single particle bound states. Therefore they are called Quasi Bound States Embedded in the Continuum, QBSEC.

2.1.3 The two body residual interaction

We now consider the full hamiltonian of the continuum shell model,

$$H = H^0 + V^{res} \ , \tag{2.7}$$

where,

$$V_{1,2}^{res} = \alpha V^0 (a + b P_{12}^{\sigma}) \delta(r_1 - r_2) \ . \tag{2.8}$$

Here, P is the spin exchange operator and α is a parameter. In our calculations $V^0 = 500 MeV$ $a = 0.73$ and $b = 0.27$. In the closed system calculations we always use

$\alpha = \alpha^{in} = 1$.

With help of the Slater determinants we write a matrix representation of this hamiltonian:

$$H_{ij} = \langle \varphi_i^{sl} \mid H \mid \varphi_j^{sl} \rangle \ . \tag{2.9}$$

Using this we numerically solve the shell model eigenvalue problem

$$H^{sm} \mid \phi_i^{sm} \rangle = E_i^{sm} \mid \phi_i^{sm} \rangle \ . \tag{2.10}$$

This gives us the shell model basis to be used later,

$$\mid \phi_i^{sm} \rangle = \sum_{j=1}^{n} a_{ij} \mid \varphi_j^{sl} \rangle \ . \tag{2.11}$$

The a_{ij} and the E_i^{sm} are real.

2.2 Coupling to the continuum

2.2.1 Projectors on subspaces

In section 2.1.3, our full Hilbert space was constructed out of bound states only, but in the following we also take into account the continuum. First we construct wavefunctions corresponding to certain decay channels:

$$\mid \chi_E^c \rangle = \mathcal{A}[\phi_{tar}(A-1)\varphi_{srlj}(1)] \tag{2.12}$$

These functions describe the residual nucleus (A-1 nucleons) in a particulary state and one particle in the continuum. We restrict our calculations to a certain number of states in the residual nucleus and emission of only one particle (a neutron in my calculations).

We have projecton operators for the two different parts of our enlarged Hilbert space:

$$Q = \sum_{i=1}^{n} \mid \phi_i^{sm}(A) \rangle \langle \phi_i^{sm}(A) \mid \tag{2.13}$$

$$P = \sum_{c} \int dE \mid \chi_E^c \rangle \langle \chi_E^c \mid \tag{2.14}$$

Q projects onto the discrete states of the excited compound nucleus and P onto the subspace of channels, consisting of the residual nucleus and one particle in a scattering state.

We have the following relations (apart from maybe a nonphysical phase),

$$P + Q = 1,\ PQ = 0,\ PP = P,\ QQ = Q \tag{2.15}$$

$$P \mid \phi_i^{sm}(A)\rangle = \mid 0\rangle \; ; \; Q \mid \phi_i^{sm}(A)\rangle = \mid \phi_i^{sm}(A)\rangle \tag{2.16}$$

$$P \mid \chi_E^c\rangle = \mid \chi_E^c\rangle \; ; Q \mid \chi_E^c\rangle = \mid 0\rangle \; . \tag{2.17}$$

2.2.2 Full solution

Next we consider the Schrödinger equation for the full continuum shell model problem,

$$(H - E) \mid \Psi\rangle = 0 \; . \tag{2.18}$$

We split the hamiltonian using $P + Q = 1$.

$$H = (P + Q)H(P + Q) = QHQ + PHP + PHQ + QHP \tag{2.19}$$

What makes the continuum shell model different from other models is that we treat all four parts of the hamiltonian with the same accuracy.

We also split the wavefunction,

$$\mid \Psi\rangle = Q \mid \Psi\rangle + P \mid \Psi\rangle \; . \tag{2.20}$$

For simplicity we define $Q \mid \Psi\rangle = \Psi_Q$, $QHQ = H_{QQ}$ and so on.

Inserting the 2.19 and 2.20 in 2.18 and multiplying to the left with P and Q respectively gives the following relations

$$(E - H_{PP})P \mid \Psi\rangle = H_{PQ}Q \mid \Psi\rangle \tag{2.21}$$

$$(E - H_{QQ})Q \mid \Psi\rangle = H_{QP}P \mid \Psi\rangle \; . \tag{2.22}$$

This is a coupled differential equation system for Ψ_P and Ψ_Q which we now solve.
Homogenous solution of 2.21 :

$$(E - H_{PP}) \mid \xi_E^{c(+)}\rangle = 0 \; . \tag{2.23}$$

Particular solution of 2.21 :

$$P \mid \Psi\rangle = \frac{1}{E^+ - H_{PP}} H_{PQ}Q \mid \Psi\rangle = G_P^{(+)} H_{PQ}Q \mid \Psi\rangle \; . \tag{2.24}$$

The function $G_P^{(+)} = P\frac{1}{E^+ - H_{PP}}P$ is the Green function in P space, i.e. the propagator in P space.

The total solution of 2.21 is

$$P \mid \Psi\rangle = \mid \xi_E^{c(+)}\rangle + G_P^{(+)} H_{PQ} Q \mid \Psi\rangle \ . \tag{2.25}$$

Equation 2.22 implies

$$Q \mid \Psi\rangle = \frac{1}{E - H_{QQ}} H_{QP} P \mid \Psi\rangle \tag{2.26}$$

Inserting 2.25 in 2.26 and solving for Ψ_Q yields

$$Q \mid \Psi\rangle = \frac{1}{E - H_{QQ} - H_{QP} G_P^{(+)} H_{PQ}} \mid \xi_E^{c(+)}\rangle \ . \tag{2.27}$$

Now we define:

$$\mid \omega_i^{(+)}\rangle = G_P^{(+)} H_{PQ} \mid \varphi_i^{sm}\rangle \tag{2.28}$$

and

$$H_{QQ}^{eff} = H_{QQ} + H_{QP} G_P^{(+)} H_{PQ} \ . \tag{2.29}$$

H_{QQ}^{eff} is the effective hamiltonian.

Using 2.20 for $\mid \Psi\rangle$, and inserting two projection operators one can show

$$\mid \Psi\rangle = \mid \xi_E^{c(+)}\rangle + \sum_{i,j=1}^{N} \left[\mid \varphi_i^{sm}\rangle + \mid \omega_i^{(+)}\rangle \right] \langle \varphi_i^{sm} \mid \frac{1}{E - H_{QQ}^{eff}} \mid \varphi_j^{sm}\rangle \langle \varphi_j^{sm} \mid H_{QP} \mid \xi_E^{c(+)}\rangle \ . \tag{2.30}$$

Changing to the representation of eigenvectors and eigenvalues of H_{QQ}^{eff}, $\mid \tilde{\Phi}_R\rangle$ and $\tilde{\varepsilon}_r$ and $\mid \tilde{\omega}_R^{(+)}\rangle$ defined in analogy with 2.28 one can show

$$\mid \Psi\rangle = \mid \xi_E^{c(+)}\rangle + \sum_{R}^{N} \left[\mid \tilde{\Phi}_R\rangle + \mid \tilde{\omega}_R^{(+)}\rangle \right] \frac{1}{E - \tilde{\varepsilon}_R} \langle \tilde{\Phi}_R \mid V^{res} \mid \xi_E^{c(+)}\rangle \ . \tag{2.31}$$

Above was used that $H_{QP} = Q V^{res} P$.

Summarising, 2.31 gives us a complete expression for the wavefunction of the continuum shell model problem. To use this formula we need to solve (apart from the bound state problem) the following three equations,

$$(E - H_{PP}) \mid \xi_E^{c(+)}\rangle = 0 \tag{2.32}$$

$$(\tilde{\varepsilon}_R - H_{QQ}^{eff}(E)) \mid \tilde{\Phi}_R\rangle = 0 \tag{2.33}$$

$$(E^{(+)} - H_{PP}) \mid \tilde{\omega}_R^{(+)}\rangle = H_{PQ} \mid \tilde{\Phi}_R\rangle \; . \tag{2.34}$$

The last equation is equivalent to $\mid \tilde{\omega}_R^{(+)}\rangle = G_P^{(+)} H_{PQ} \mid \tilde{\Phi}_R\rangle$.

The $\tilde{\varepsilon}_R$ are complex because H_{QQ}^{eff} is non-hermitean and thus we define:

$$\tilde{\varepsilon}_R(E) = \tilde{E}_R(E) - \frac{i}{2}\tilde{\Gamma}_R(E) \; . \tag{2.35}$$

Note also that the eigenfunctions of H_{QQ}^{eff} can be represented as a linear combination of the eigenfunctions of H_{QQ},

$$\mid \tilde{\Phi}_i\rangle = \sum_{j=1}^{N} b_{ij} \mid \varphi_j\rangle \tag{2.36}$$

where the coefficients b_{ij} are complex. It holds $|\varphi_i|^2 = 1$ while $|\tilde{\phi}_i|^2 \geq 1$. In the numerical calculations the bound state problem is solved only once with $\alpha = \alpha^{in} = 1$ in 2.8. In the investigations we vary α^{ex}, which is the parameter for the residual interaction V for the continuum hamiltonian. Varying α^{ex} thus is equivalent to varying the strength of H_{PQ} and H_{QP}, i.e. the strength of the mixing between the two subspaces.

2.2.3 Cross section

The experimentally measurable value we can calculate in this model is the cross section.

First derive the S-matrix.

In [18] the S-matrix is defined as follows:

$$S_{cc'}(E) = exp(2i\delta_c)\delta_{cc'} - 2i\pi\langle\chi_{E'}^{c'(-)}|\hat{V}^{Res}|\Psi_E^{c(+)}\rangle \; . \tag{2.37}$$

Also define

$$\tilde{\gamma}_{Rc} = \frac{1}{\sqrt{2\pi}}\langle\xi_E^{c(-)}|V^{Res}|\tilde{\Phi}_R^r\rangle \; . \tag{2.38}$$

The partial width of a resonance is $\Gamma^c = \mid \tilde{\gamma}_{Rc} \mid^2$ [18].

One can show

$$S_{cc'} = S^{(1)}_{cc'} + S^{(2)}_{cc'} \; . \tag{2.39}$$

where

$$S^{(1)}_{cc'} = exp(2i\delta_c)\delta_{cc'} - 2i\pi \langle \chi^{c'(-)}_{E'} | \hat{V}^{Res} | \xi^{c(+)}_{E} \rangle \tag{2.40}$$

and

$$S^{(2)}_{cc'} = i \sum_R \frac{\tilde{\gamma}_{Rc'}\tilde{\gamma}_{Rc}}{[E - \tilde{E}_R + \frac{i}{2}\tilde{\Gamma}_R]} \; . \tag{2.41}$$

The first term $S^{(1)}_{cc'}$ describes all processes that can take place without coupling to the Q-space. This is called the direct reaction part. The second part $S^{(2)}_{cc'}$ desribes the possibility of creation and decay of a compound nucleus in the states R, i.e. the resonant part [18].

The S-matrix gives the cross section

$$\sigma^{tot} = \frac{\hbar^2\pi^2}{2mE} \mid 1 - S \mid^2 \; . \tag{2.42}$$

E und m are energy and mass of the incoming particle.

The S-matrix is unitary and thus $\mid S_{cc'} \mid \leq 1$.

In the case of isolated resonances is a simple way to study the cross section to find the poles of the S-matrix. From 2.39 and 2.41 we can see that the complex poles of the S-matrix are at the energy values of the fixpoint solutions,

$$\tilde{E}_R(E = E_R) = E_R \; . \tag{2.43}$$

E_R and $\Gamma_R = \tilde{\Gamma}_R(E_R)$ describes energy and width of a resonance.

It should be noted that as $\tilde{\varepsilon}_R$ is energy dependent E_R and Γ_R do not give all the information about the shape of isolated resonances. In the case of high level density apart from this also different kinds of interference effects will take place.

2.2.4 Some final comments

The wavefunctions of the resonant part of Ψ consist of two parts, $\mid \tilde{\Phi}_i \rangle$ and $\mid \tilde{\omega}^{(+)}_i \rangle$. The $\mid \tilde{\omega}^{(+)}_i \rangle$ functions are important. They have an overlap to the channel wave functions and thus describe the fact that when we couple the QBSEC to the continuum, the corresponding states can decay.

Note also that the non-hermitean part of the effective hamiltonian is $QHP * G_P * PHQ = QVP * G_P * PVQ$. As the strength of V is governed by the parameter α^{ex}, increasing α^{ex} means increasing the non hermitean part by about $(\alpha^{ex})^2$. The non-hermitean part is responsible for the eigenvalues beeing complex. Therefore when we increase α^{ex} we expect the imaginary part of the eigenvalues of the effective hamiltonian H^{eff}_{QQ} to increase.

2.3 S-matrix-model

For a part of the discussion a simple S-Matrix model has been used [18]. N bound states and K open decay channels couple to the bound states $\mid \Phi_i\rangle$. The hamiltonian is

$$\mathcal{H} = \sum_{i,j=1}^{N} |\Phi_i\rangle \hat{H}^0_{ij} \langle \Phi_j| + \sum_{c=1}^{K} \int dE |\chi^c(E)\rangle E \langle \chi^c(E)| + \sum_{c=1}^{K} \sum_{i=1}^{N} \int dE \Big[|\Phi_i\rangle V^c_i(E) \langle \chi^c(E)| + h.c. \Big]. \tag{2.44}$$

By derivation of the S-matrix an effective hamiltonian, that describes the poles of the S-matrix, can be defined. Far from thresholds the coupling vectors can be considered as energy independent and for time invariant processes they can be chosen real. The effective hamiltonian for this model is then

$$H^{eff} = \hat{H}^0 - i\pi \cdot VV^+ \; . \tag{2.45}$$

V can be choosen in an arbitrary way, and thereby the coupling strength of different states to a certain decay channel can be controlled. Also H^0, that describes the result of the internal mixing and which is diagonal, can be choosen in an arbitrary way.

Chapter 3

SUMMARY OF SOME RELEVANT RESULTS

The aim of this chapter is to give a brief summary of some earlier results which are important for the interpretation of the results obtained when including threshold effects [5-7, 11-16].

3.1 The trapping effect in an ensemble far from threshold

An ensemble of 70 states with quantum numbers $J^\pi = 1^-$ and energy between 22 and 44MeV has been investigated for two open channels in [6]. The energy of the system, E_{lab}, is chosen to be constant (34.7Mev). The parameter α^{ex} for the strength of the residual interaction that couples the bound states to the continuum was varied in [6] between 0 and 10. The experimental value of α^{ex} is between 1 and 2. As the nuclear force increases we expect the width of the resonances to increase. Thus increasing α^{ex} means increasing $\frac{\Gamma}{D}$, where Γ is the average width and D the average distance of the resonances. The aim of the investigations was to study the same states under different conditions and thus α^{in} was always 1. The eigenvalue picture was studied, i.e. the real and imaginary parts of the eigenvalues of the effective hamiltonian 2.29 were plotted shown in the same plot for all α^{ex}.

The main features of the eigenvalue picture of the ensemble considered are as follows. As α^{ex} increases from zero so do the widths of all the resonances. At a critical value of α^{ex}, that lies between 2 and 3, the widths of two resonances start to increase rapidly whereby the widths of all the other ones decrease. This effect is called trapping. At still larger α^{ex} a hierarchically order is formed, i. e. some of the trapped states can be slightly broader at the expense of some other states. The number of broad states is exactly equal to the number of open decay channels.

The two broadest states expire a large shift in their energy position. When these states are shifted far away from the region where the remaining states are lying, two new states can become broad (second generation) and so on [6].

In [6] it is also shown that the value $\mid \tilde{\Phi}_r \mid^2$ becomes large whenever two states get into 'conflict' with each other. Conflict means that two states, for a given α^{ex}, are very close to each other in the complex eigenvalue plane. For a slightly larger α^{ex}, the two states have 'decided' which is to 'win'. One of them gets trapped and the other one can grow broader. The $\mid \tilde{\Phi}_r \mid^2$ decrease to values close to one (in the closed system with the hermitean operator H_{QQ}, this value is normalized to one).

What is described above are the general features of the trapping effect. It is also called slaving principle and is an example of selforganization in the nuclear system.

3.2 The tail and the cusp

To consider $\tilde{\varepsilon}_i = \tilde{E}_i(E) + \frac{i}{2}\tilde{\Gamma}_i(E)$ as a function of energy gives rise to some new features when considering isolated resonances. It is generally not true that we can explain the resonant part of the cross section by writing Breit-Wigner shapes at the positions of the poles of the S-matrix (corresponding to the fixpoint solutions 2.43 of the effective hamiltonian).

In [5], pp 648, the shape of a single resonance close to the opening of an inelastic decay channel is investigated. As usual the width $\tilde{\Gamma}_R(E)$ of the resonance rises strongly at the threshold energy.

Consider a resonance with fixpoint solution energy slightly below the threshold. There it has a small width. If one calculates the complex energy eigenvalue for an energy slightly above the resonance, the imaginary part, corresponding to the width, will be larger. The cross section thus 'sees' a broader peak from above the threshold and in the cross section these two pictures have to be 'fitted', giving rise to an unsymmetric resonance shape showing a long tail to higher energies.

If a resonance happens to lie exactly at the threshold energy the cross section 'sees' two pictures at the same point: a narrow peak for energy going down and a broad peak for energy going up. These two pictures are 'fitted' giving rise to a 'cusp' in the cross section.

The energy dependence of the complex eigenvalues thus implies strange features in the cross section for single resonances. This is a justification for looking at these eigenvalues not only at the fixpoint solutions.

3.3 Interference phenomena for overlapping resonances

The cross section can be calculated from the S-matrix with 2.42. Due to the unitarity of the S-matrix (implying $\mid S \mid \leq 1$) the cross section can not be arbitrarily large. Therefore one can not simply add the contributions from the single overlapping resonances to reproduce the cross section, but different kinds of interference phenomena occur.

If one has large broade states surrounded by smaller narrow ones, the smaller ones are often visible as dips instead of peaks in the cross section. This is caused by the fact that the broade state has already reached almost the maximum value for σ^{tot}.

Finally it should be noted that in the case of more than one open decay channel and high level density, the trapped states are not visible as narrow resonances in the cross section but as fluctuations [5].

3.4 Level repulsion

The trapping effect can be considered as an avoided resonance overlapping in analogy to avoided level crossing of discrete states [14]. As long as $\frac{\Gamma}{D}$ approaches unity all the resonances becomes broader (Γ and D defined as in section 3.1). For $\frac{\Gamma}{D} \geq 1$ a redistrubution takes place giving almost all of the sum of the widths to a small number of states (two in the case of two open decay channels) so that the widths of the trapped states start to decrease. Even though the broad states overlap many of the smaller ones, the smaller states will almost not overlapp their narrow neighbours.

We can also see level repulsion in the eigenvalue picture. When two states are getting close in this picture (for a certain α^{ex}) they come into conflict and for slightly larger α^{ex} one of the two states will be trapped and the other can grow broader. The point is that the two resonances will avoid each other. This can be intuitively understood if we consider the complex eigenvalues as the poles of the S-matrix [14]. The pole corresponds to a whole mountain in the S-matrix landscape. Obviously it is unfavourable for the system to manage a 'penetration' of these mountains.

3.5 Order and chaos

Trying to characterize the wavefunctions of a system as ordered or chaotic is difficult. Using the degree of mixing versus a certain (intuitive) basic set has the disadvantage of being basis dependent. One can often find another basis relative to which the mixing is smaller. In [5], pp 671, the proposal is made that both level repulsion and high degree of mixing characterize chaos.

The mixing of the complex wavefunctions versus the Slater determinants or versus the states of the corresponding closed system (shell model states) is investigated in [7]. For small α^{ex} the wavefunctions of the open system can be approximated with the wavefunctions of the closed system. The system is ordered and the information entropy is low. As α^{ex} approaches the critical value a redistrubution takes place. All the wavefunctions of the states in the open system are mixed in the representation of the wavefunctions of the closed system. The system is chaotic and the information entropy approaches a maximum. Level repulsion occurs. The spectroscopic information of the closed system is lost.

This transition to chaos however is accompanied by the formation of a new order. If one wants to describe the closed system one has to take into account all the states (70 in the paper [7]). If one wants to give a relevant description of the open system at high level density and short timescales however, it is sufficient to describe the broad states (2 in [7]), because we will not see the long lived states. Thus the relevant information entropy decreases. This is the reason why we call trapping a selforganizing effect. The total information entropy however increases and thus no 'thermodynamical laws' are broken.

The open system is also ordered in yet another way. In the closed system representation, the broad modes are strongly mixed. In the channel wavefunction representation however, they are almost completely pure due to their strong coupling to one of the channels respectively. This is a consequence of the fact that a broad state has a short lifetime, which implies a large overlap to a decay channel.

Chapter 4

AN ENSEMBLE CLOSE TO THE ELASTIC THRESHOLD

In our investigations [6][7][5], the solving of the closed shell model problem is made in a special program writing data to files. These datafiles define our operator H_{QQ} with eigenfunctions, eigenvalues and also the matrix elements of the operator H_{QP}. We can alter the eigenvalues in an arbritrary way keeping all the other data unchanged before solving the continuum shell model problem. This gives rise to a new completely legal matrix representation of an operator, still called H_{QQ}, but we can not write an analytical expression for it, and to what extent this operator has anything to do with nuclear physics is a question for the discussion.

In previous calculations [6] the behavior of a 2p-2h QBSEC ensemble with 190 members and $J^\pi = 1^-$ at the calculated energies between 20 and 45 MeV for the Q-value 12.691 MeV was investigated. This is well above both the elastic threshold (at 0 MeV) as well as the first inelastic threshold at 6.149 Mev. These two channels were the only channels considered in the calculations. Both channels are really open because the system energy is well above both thresholds. Scattering of protons on ^{15}N was considered.

To investigate threshold effects we used the same ensemble and decreased the real energy eigenvalues of H_{QQ} by e.g. 25 MeV. The new closed system energies, complex eigenvalues of the effective hamiltonian and so on are marked with a prime. A simple way to justify this shift is to note that it is simply equivalent to increasing the Q-value. In our calculations also the Q-value, which is defined as the energy difference between the ground state of the compund nucleus and the elastic threshold, is increased by e.g. 8 MeV.

In many of the calculations the eigenvalues of the effective hamiltonian 2.29 were calculated at a certain fixed energy $E = E_{lab}$ of the system. It is important to remember that we do not solve the fixpoint equation. Therefore statements can only be made about the real and imaginary part of these eigenvalues.

The off-diagonal elements of H_{PP} describe the fact that the channels also couple to each other. Therefore a state that is decoupled from a certain decay channel can still feel the opening of that channel. To investigate this feature the channel-channel coupling can be turned off in the program, i.e. the off diagonal elements of H_{PP} can be forced

to be zero. Unless otherwise stated the calculations are performed with channel-channel coupling on.

4.1 Numerical results for the ensemble

This chapter describes the results of a series of calculations made with the same ensemble as used in [6]. It has 190 members of 2p-2h nuclear structure and $J^\pi = 1^-$. For a Q-value of 20.196 MeV it has QBSEC energies of between 10 and 45 MeV. The experimental Q-value is 12.691 MeV. Elastic neutron scattering was always considered (E=0 MeV) and in a few cases also inelastic scattering with the threshold at $E^*_{thr} = 6.149$ MeV.

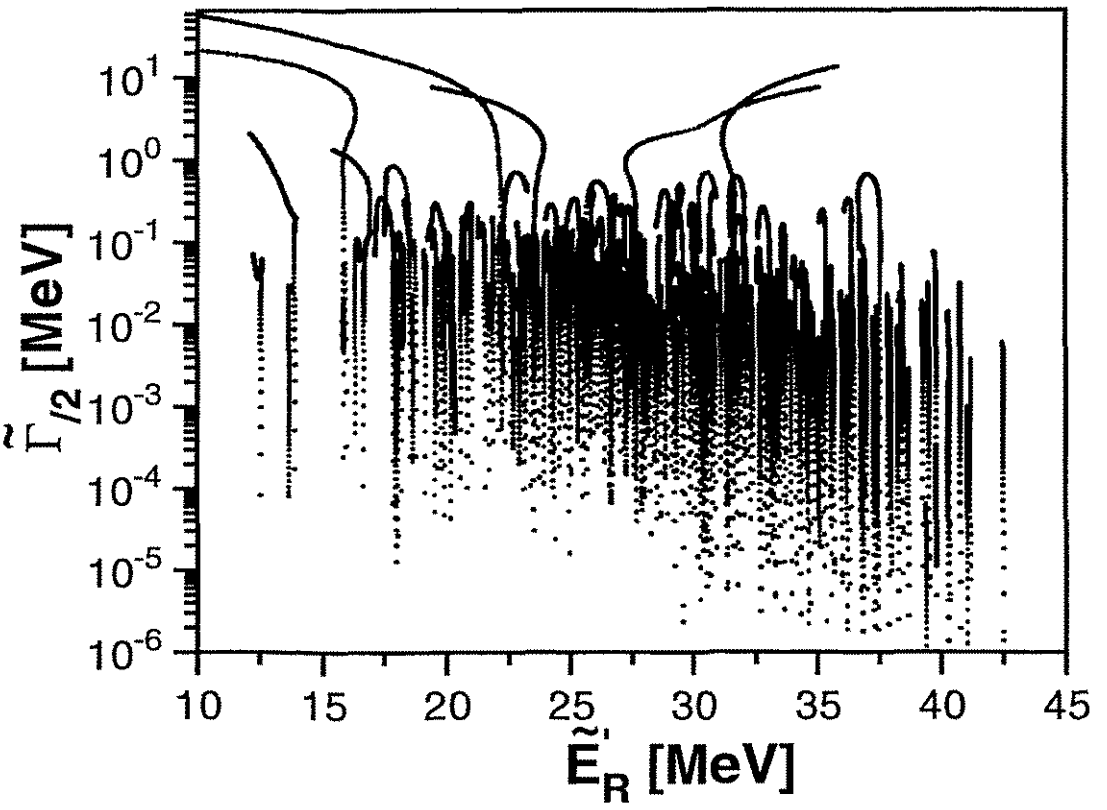

Figure 4.1: The eigenvalue picture for 190 resonances and 2 neutron channels by varying α^{ex} from 0.05 to 8.65 in steps of 0.05. $E_{lab} = 29$ MeV, $Q = 20.691$ MeV, $E^* = 6.149$ MeV and $E'_{sm} = E_{sm}$.

4.2 Original ensemble

For later comparison the eigenvalues of the ensemble at its original place far from thresholds was calculated for α^{ex} varied from 0.05 to 8.65 in steps of 0.05. $E_{lab} = 29$ MeV, $Q = 20.691$ MeV, $E^*_{thr} = 6.149$ MeV, and $E'_{sm} = E_{sm}$ (Fig. 4.1). For small α^{ex} there is a spectroscopical slope which is removed for large α^{ex} (eg 5) by the trapping effect. The

first two broad states arise from the lower part of the spectrum.

4.3 Cross section without tail

In fig. 4.2 a cross section for $\alpha^{ex} = 1.5$, Q-value=20.691MeV, $E'_{sm} = E_{sm} - 25MeV$ and one neutron channel is shown. The values are chosen so that the negative states close to the elastic threshold are trapped.

In the cross section we can see a narrow resonant state close to the threshold and a small tail with interference effect from a narrow negative state close to threshold.

4.4 Cross section showing a 'tail' from a discrete state

A cross section with $\alpha^{ex} = 2.5$, Q=8.391 MeV, one neutron channel and $E'_{sm} = E_{sm} - 25MeV$ is shown in fig. 4.3b. In the corresponding eigenvalue picture (fig. 4.3a) we can see that the broadest state lies just below the elastic threshold. We can not solve the fixpoint equation 2.43 for this resonance because the border conditions for neutron scattering inherent do not allow for a solution at negative system energies. Furthermore, three trapped states slightly above zero were deleted to make the situation clearer.

The resulting cross section has much larger values close to $E_{lab} = 0$ than the direct part although there is no broad resonance close to this energy. This difference shows the influence of the negative state that would be a resonance if the Q-value would be slightly higher.

4.5 Varying E_{lab} for fixed α^{ex}

In this series of calculations (figs. 4.4 and 4.5) the energy E_{lab} of the system was varied while α^{ex} was fixed to $\alpha^{ex} = 1$ and 4 respectively. $E'_R = E_R - 25$ MeV, and E_{lab} is varied from 0.01 MeV to 8.2 MeV in steps of 0.05 MeV. $E^* = 6.149$ MeV. Channel-channel coupling is both turned on and off. The common features for all plots shown are that the opening of the inelastic threshold enables an extra state to become broad. The first broad state is still the broadest one after the opening of the second threshold. For $E_{lab} \to 0$ all $\tilde{\Gamma}_R \to 0$.

For $\alpha^{ex} = 1$ a change in the derivative can be seen at the inelastic threshold for the first broad state for both channel-channel coupling on and off (fig 4.4a and b). This implies that the broadest state is not almost completely coupled to only one channel. In the eigenvalue picture (fig. 4.5a) almost no trapping can be seen. There is a slope in the width of this picture; for all energies the $\tilde{\Gamma}_R$ of the states at larger resonance energies are smaller than the $\tilde{\Gamma}_R$ of states at lower energies. The real part of the eigenvalues of H^{eff}_{QQ}, $\tilde{E}_R$, are almost independent of the system energy, E_{lab}, for most of the states.

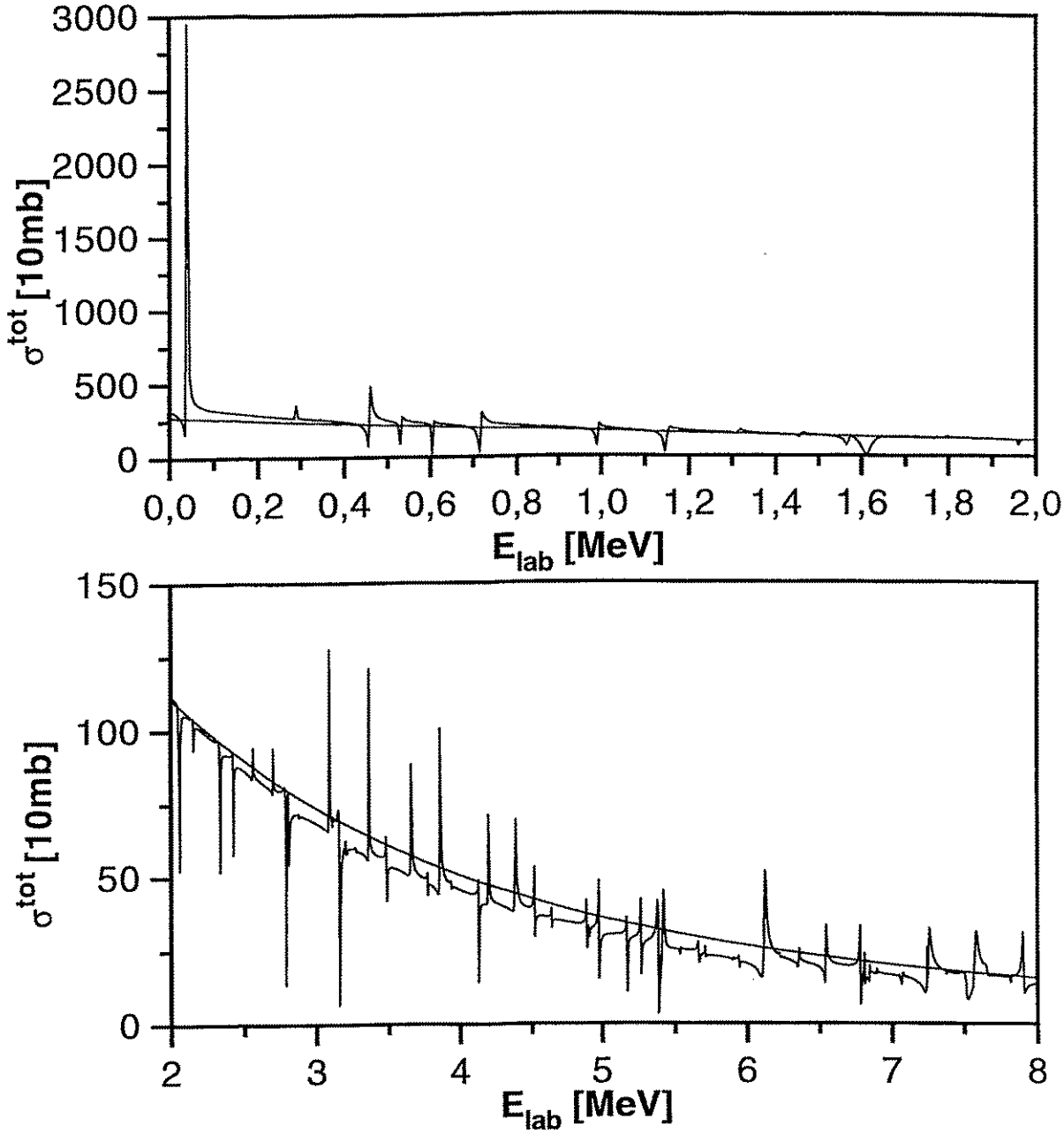

Figure 4.2: Cross section for $\alpha^{ex} = 1.5$, Q-value=20.691 MeV, $E'_{sm} = E_{sm} - 25$ MeV , one neutron channel.

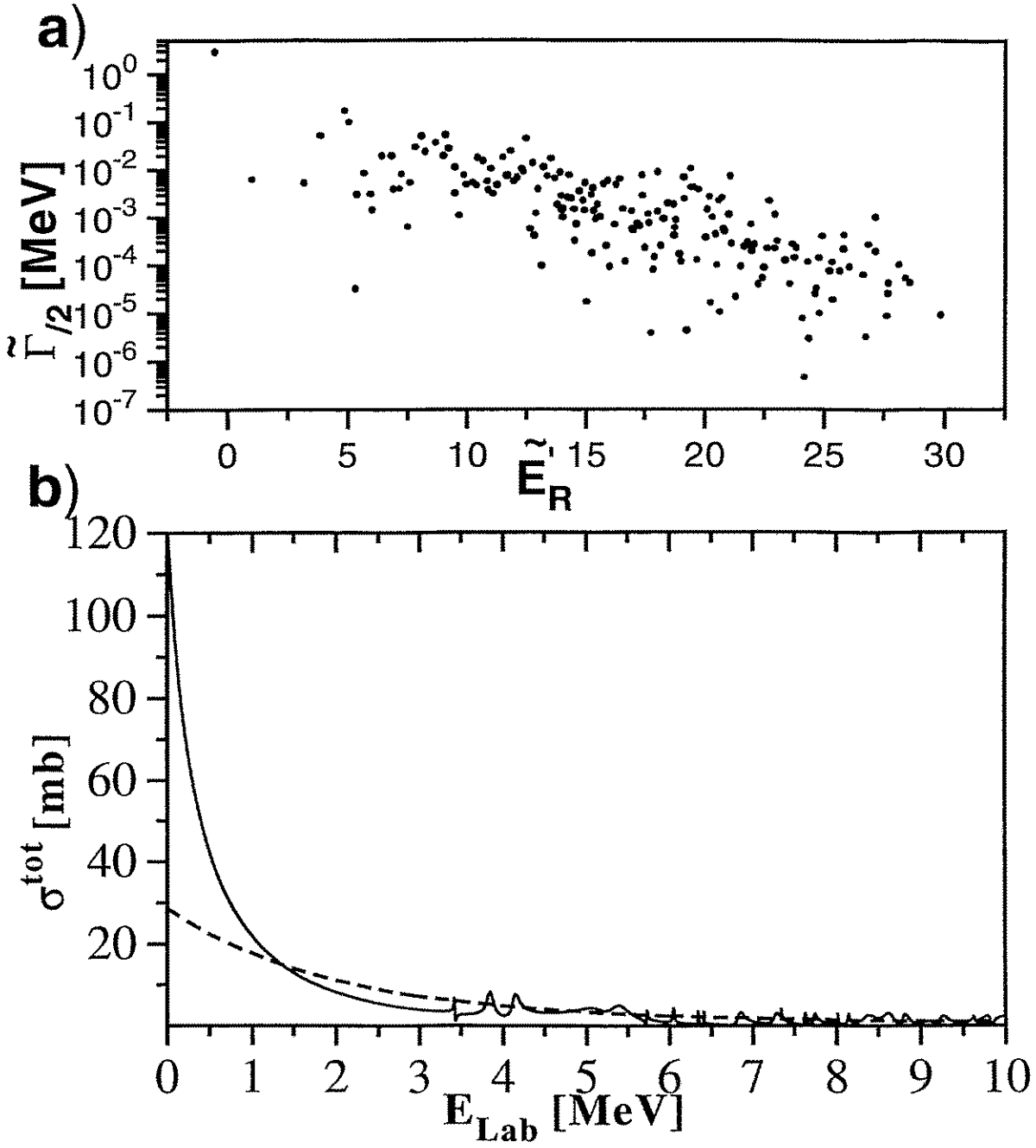

Figure 4.3: The imaginary parts $\frac{\tilde{\Gamma}_R}{2}$ of the 190 states for $\alpha^{ex} = 2.5$, Q=8.391 MeV, $E'_{sm} = E_{sm} - 25$ MeV for one neutron channel (a) and the corresponding cross section (b).

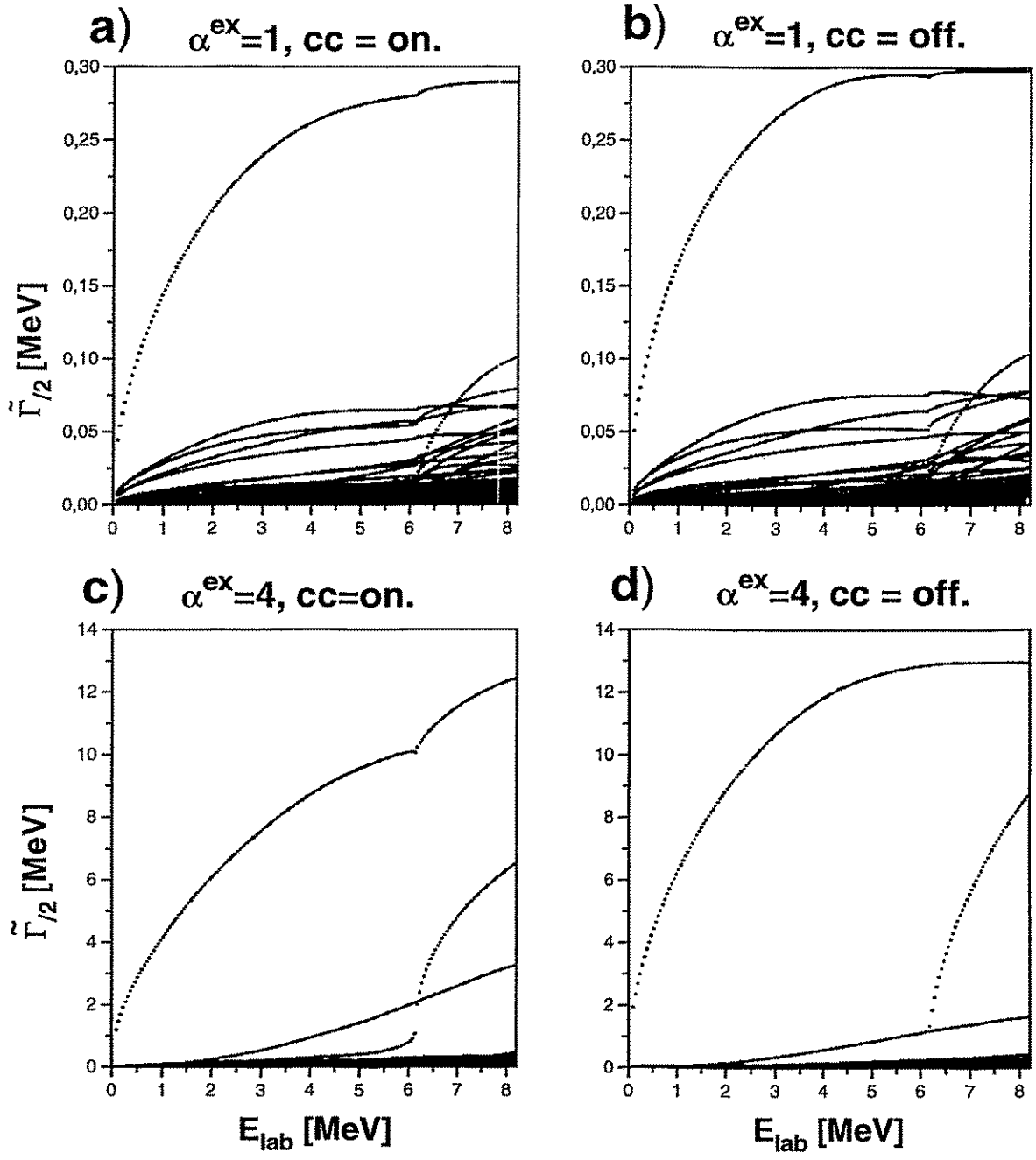

Figure 4.4: The imaginary parts of the eigenvalues of H_{QQ}^{eff} as a function of E_{lab} for α^{ex}=1 and 4, Q=20.691 MeV, $E^* = 6.149$ MeV and $E'_R = E_R - 25$ MeV.

A very pure example is shown for $\alpha^{ex} = 4$. For channel-channel coupling off, the first broad state does not notice the opening of the second channel (fig. 4.4c), which implies that the state is almost purely coupled to the first channel. The slope in the width is still there. Trapping and energy shift of the low-lying states occur (4.5b). There is also a third broad state, which is significantly broader than the trapped states but narrower than the first broad state and also narrower than the second broad state after the inelastic threshold has opened. This third state does not feel the inelastic threshold. $\tilde{E}_r(E)$ is almost constant for all but the broadest states.

Finally and quite obviously the maximum for the width of the broadest states increases strongly with increasing α^{ex}. It is approx. 0.3 and 13 respectively for the two considered cases.

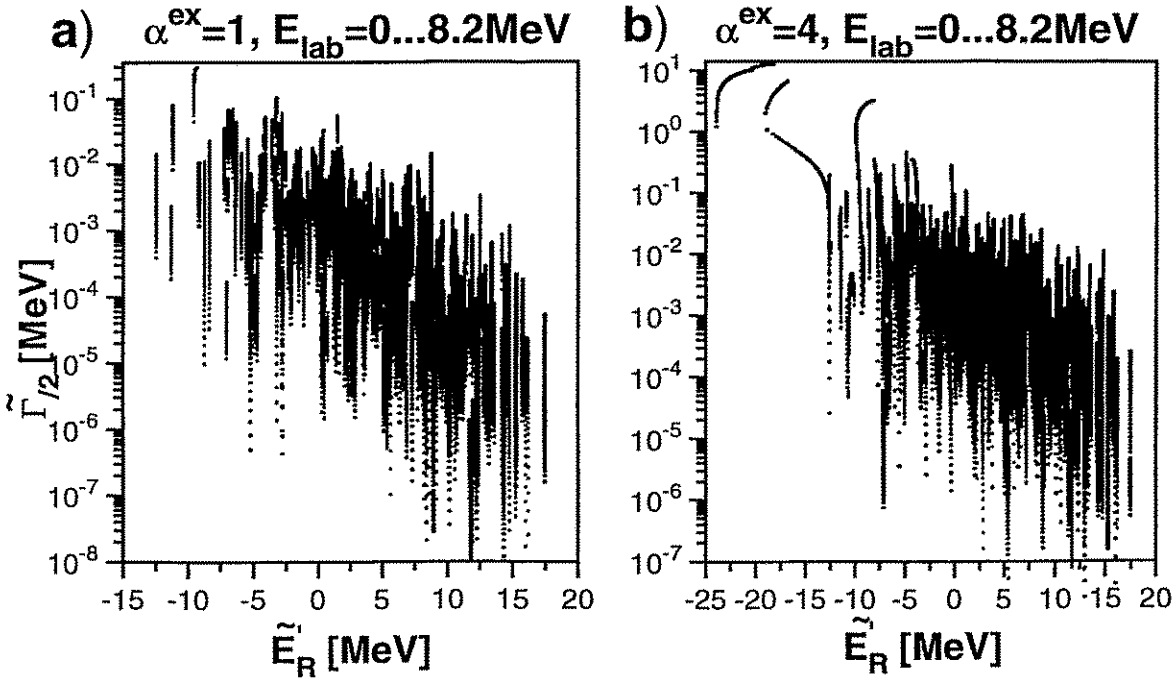

Figure 4.5: Eigenvalue picture for 190 resonances by varying E_{lab} from 0 to 8.2 MeV for α^{ex}=1 and 4. Q=20.691 MeV, E^*_{thr}=6.149 MeV and $E'_R = E_R$-25 MeV. Channel-channel coupling is on.

4.6 The ensemble around zero

In these calculations, the following values are used: $E_{lab} = 4$ MeV, $E'_R = E_R - 25$ MeV, $Q = 20.691$ MeV and only one open channel. α^{ex} is varied from 0.05 to 8.65 in steps of 0.05 (fig 4.6).

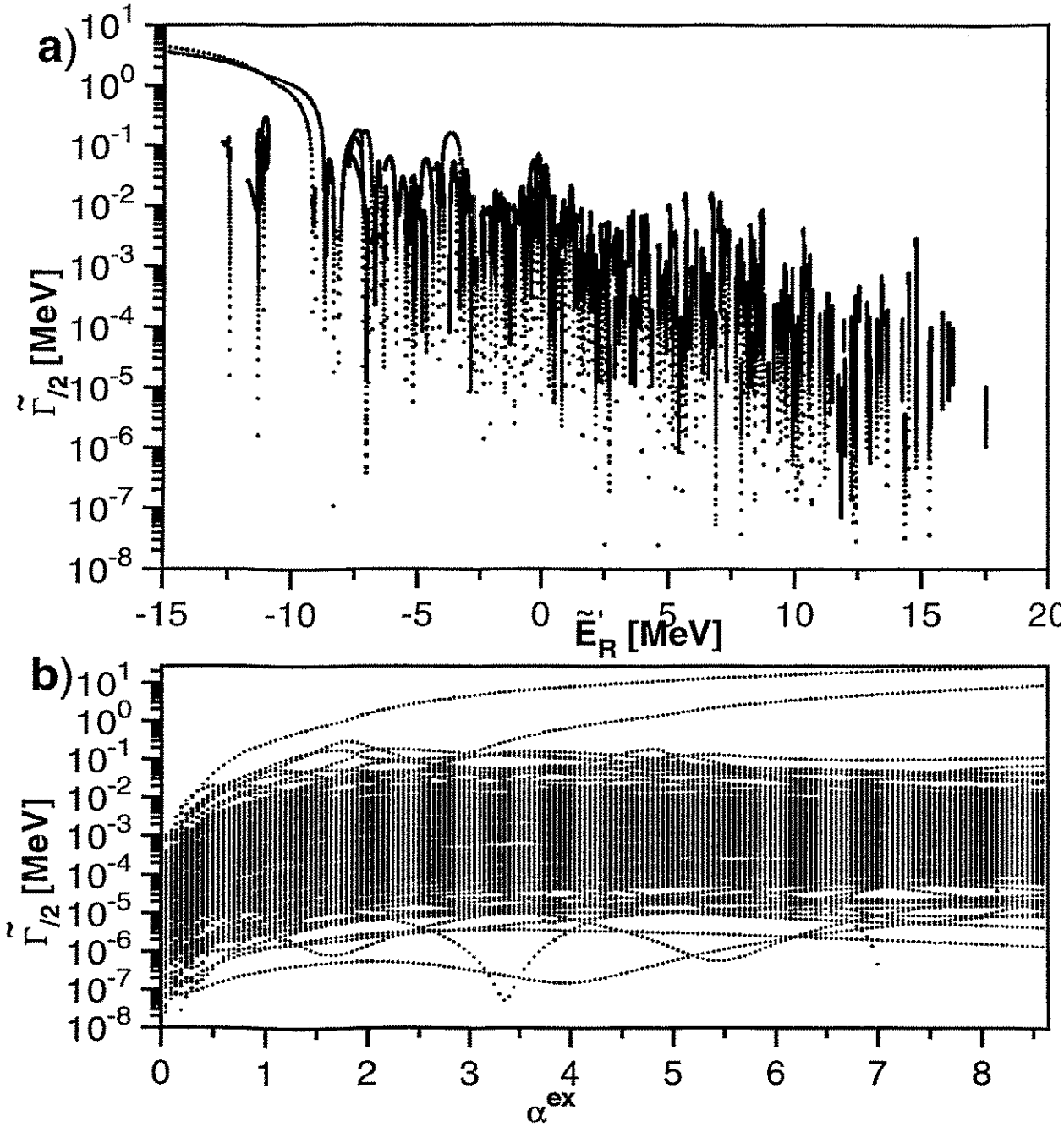

Figure 4.6: Eigenvalue picture for 190 states by varying α^{ex} form 0.05 to 8.65 in steps of 0.05(a) and $\tilde{\Gamma}_R$ as a function of α^{ex} (b), $E_{lab} = 4$ Mev, $E'_R = E_R - 25$ MeV, $Q = 20.691$ MeV and one neutron channel.

The general features of the eigenvalue picture (fig 4.6a) are as follows: For very small α^{ex} there is a global structure in the shape of the ensemble. The $\tilde{\Gamma}_R$ of the resonances lying at higher E'_R are smaller by several orders of magnitude than those of the resonances at smaller energies. The range of the energies is from -15 to 15 MeV. As α^{ex} increases the $\tilde{\Gamma}_R$ of all the resonances increase, but the slope remains visible. Trapping only occurs for small resonance energies (i.e large $\tilde{\Gamma}_R$), which corresponds to negative states for the Q-value chosen. The broad states (one in every generation) also come from this lower part of the spectrum, and their $\tilde{E}'_R$ escape to very low energies. As α^{ex} approaches 8.65, the slope is still there, but some trapping starts to occur also for states with higher energy eigenvalues.

In the plot of $\tilde{\Gamma}_R$ versus α^{ex} (fig 4.6b) two generations with one member each can be seen.

4.7 Varying α^{ex} for E_{lab}=15 MeV

In this calculation, two channels are open and E_{lab} is increased to 15 MeV but all other values are unchanged in comparison with section 4.6 (Fig. 4.7.)

At $E_{lab} = 15$ MeV, one can clearly see that some extra states get broad, corresponding to the opening of the second channel. The slope in the eigenvalue picture is still there, but it is less pronounced than in fig. 4.6. The new broad modes appear in the middle of the energy range of the ensemble. Therefore we can see trapping also in the higher energy region. We see two members in most of the generations. It should be noted however, that the rule according to which the number of broad modes should be equal to the number of open decay channels is strict only for the first generation.

4.8 The ensemble with an energy gap

For all resonances of section 4.6 with $E'_R < 0$, the E_R was decreased by 3 MeV while for all other states the energy was increased by 5 MeV (Fig 4.8). This splits the ensemble into a negative and a resonant part.

For small α^{ex} this enables the lower lying resonances in the resonant part of the ensemble to become broad and to trap the rest of the resonant states. As α^{ex} grows, so does the $\tilde{\Gamma}_R$ of all the states. For sufficiently large α^{ex} it can clearly be seen that the broadest of the resonant states gets trapped. This trapping occurs obiously due to the discrete states.

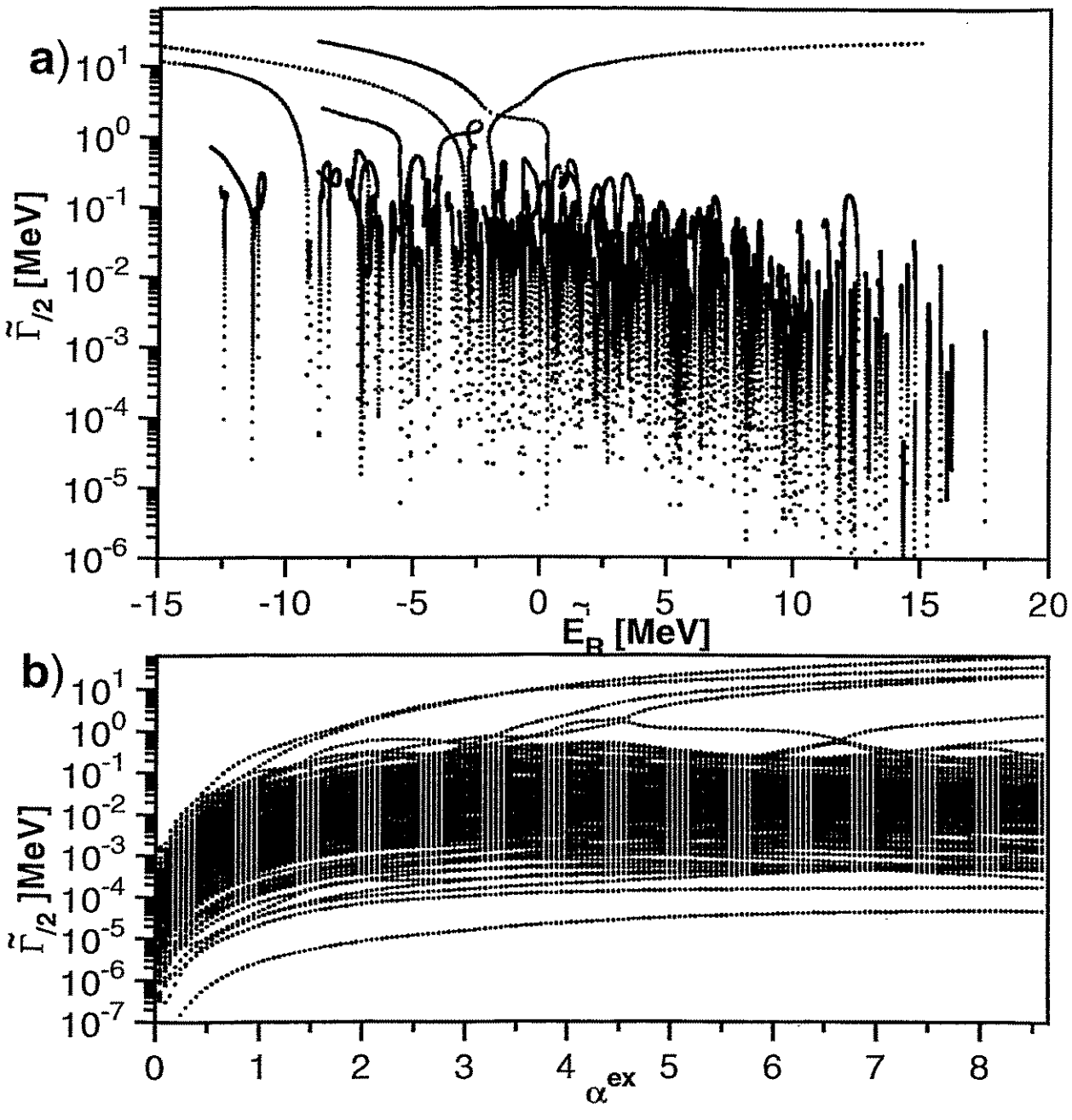

Figure 4.7: Eigenvalue picture for 190 states when varying α^{ex} from 0.05 to 8.65 in steps of 0.05(a) and $\tilde{\Gamma}_R$ as a function of α^{ex}(b) for $E_{lab} = 15MeV, E'_R = E_R - 25$ MeV, $Q = 20.691$ MeV, and two neutron channels.

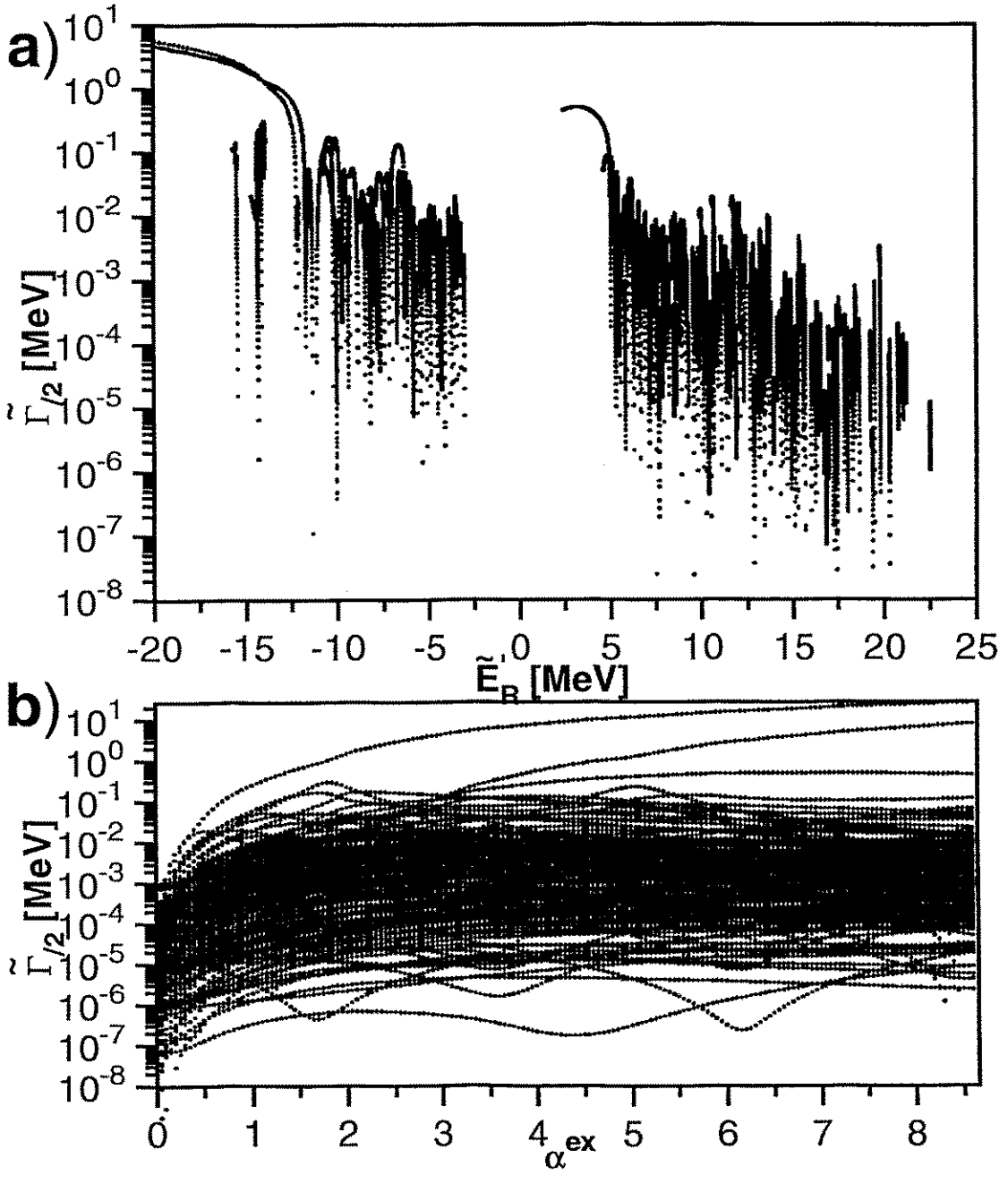

Figure 4.8: The eigenvalue picture for $E_{lab} = 4$ Mev and α^{ex} varied from 0.05 to 8.65 in steps of 0.05 with a gap introduced around $\tilde{E}'_R = 0$(a) and $\check{\Gamma}_R$ versus α^{ex}(b) $Q = 20.691$ MeV, $E'_R = E_R - 25$ MeV, one neutron channel

4.9 Energy reversal of the ensemble

To see if the slope in the widths of fig. 4.6 is purely an effect of the internal structure or also an effect caused by the variation in resonance energy we simply swapped the energies of the unperturbated states around the center of the ensemble (Fig. 4.9).

This gives rise to two different regions for α^{ex}. For small α^{ex} the slope is reversed. This implies that the slope for small α^{ex} is caused by the internal structure of the states.

As α^{ex} approaches 5 however, the $\tilde{\Gamma}_R$ of states at small resonance energies grow faster than the gamma values for states at higher resonance energies. This results in the fact that for $\alpha^{ex} = 5$ there are trapped states in the whole ensemble and the $\tilde{\Gamma}_R$ of all the trapped states are of the same order of magnitude. The first broad state comes from the higher energy region, but the rest comes from the lower energy regions.

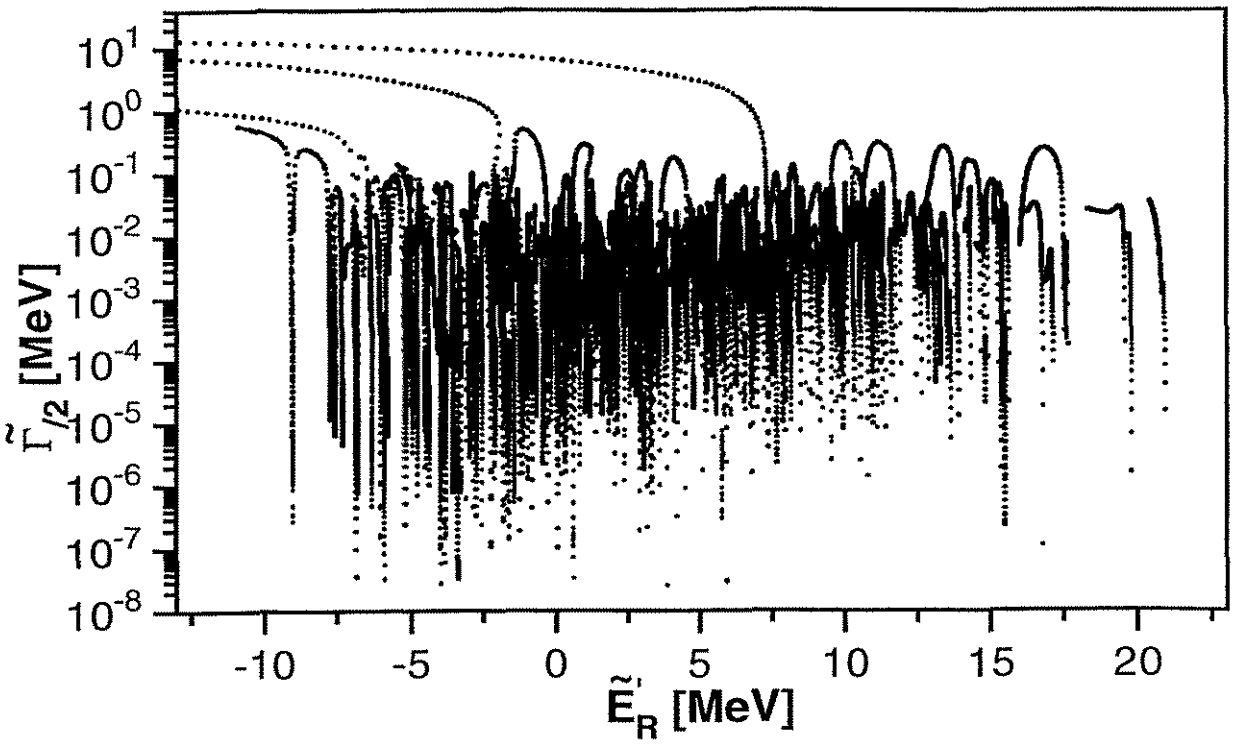

Figure 4.9: The eigenvalue picture for α^{ex} varied from 0.05 to 8.65 in steps of 0.05 for $E_{lab} = 4$ MeV and E'_R swapped around the center. $E'_R = E_R - 25$ MeV, $Q = 20.691$ MeV and one neutron channel.

4.10 Cross section of two states around $E_{lab} = 0$ MeV

To make things as simple as possible, we have investigated the cross section of a system with only two resonances. One of the resonances is just below the elastic threshold and one slightly above (fig. 4.10). Curve (c) shows the cross section calculated with only the negative state. One can see the tail when comparing with the direct part (curve d). Curve (a) is the cross section calculated with only the resonant state, which shows an interference minimum for low energies. Curve (b) shows the interference effect for the cross section calculated with both the states. The influence from the negative state removes almost completely the effect of the resonance in the very neighbourhood of the elastic threshold. What still can be seen is an interference minimum followed by a peak and the tail of the resonance. Obviously, the two states repulse each other.

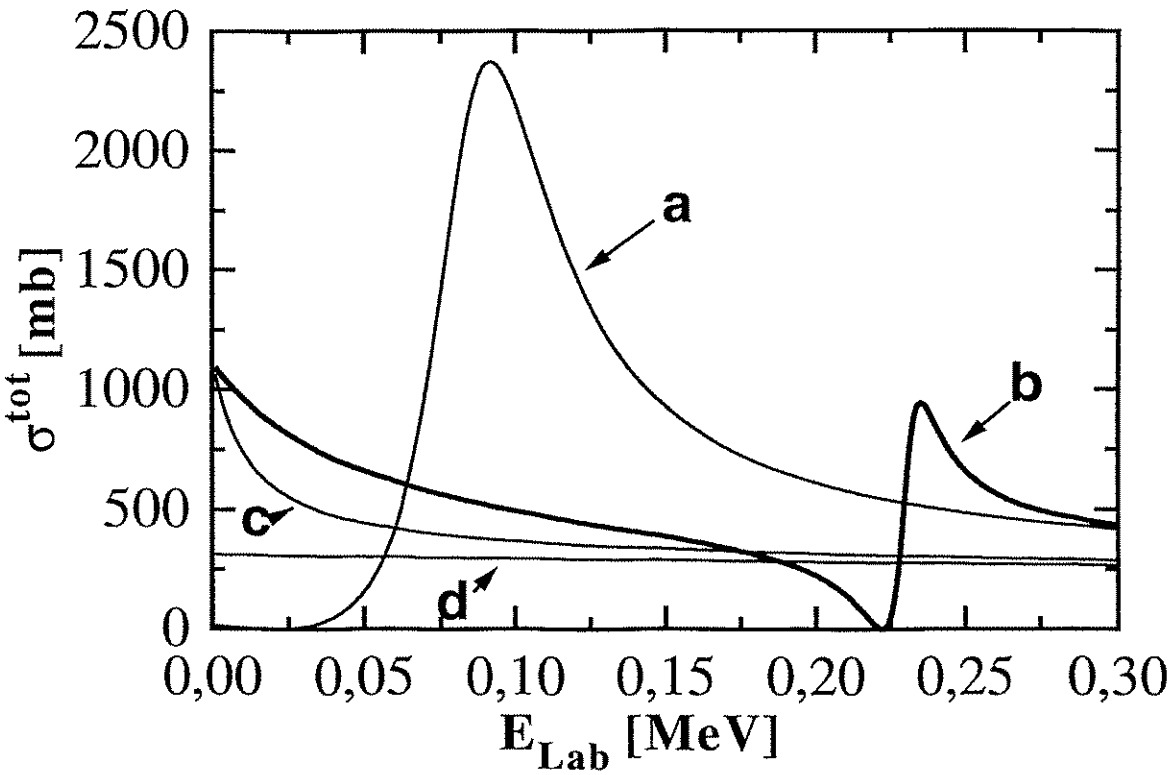

Figure 4.10: Interference in the cross section between one negative state (at -0.07 MeV) and a resonant state (at 0.7 MeV). Curve (a) shows the resonant state without any interference and curve (b) shows the interference between the two states. Curve (c) shows the tail of the negative state and curve (d) the direct part.

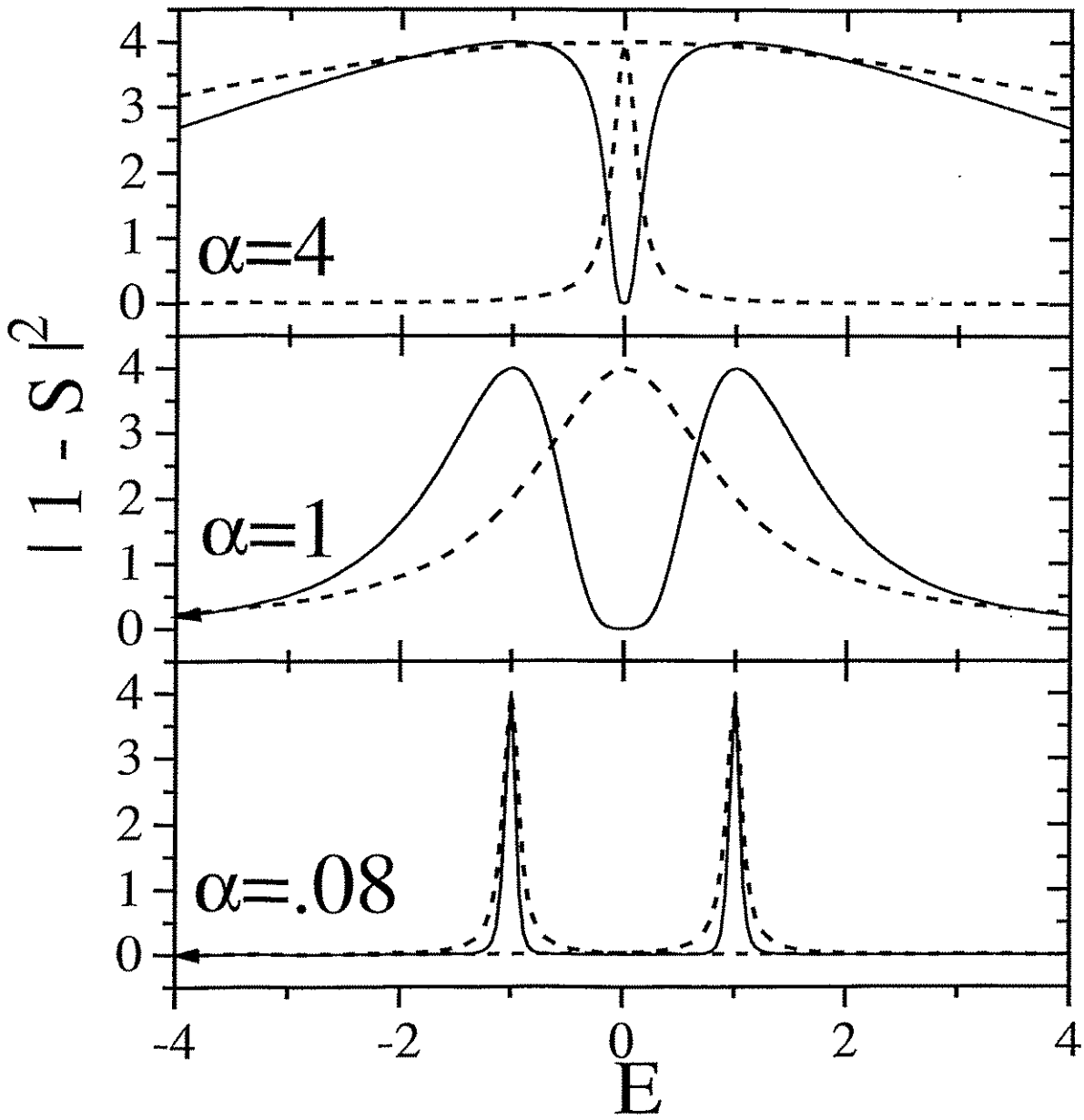

Figure 4.11: Interference in the S-matrix model for two states at different α^{ex}. The corresponding Breit-Wigner shapes are shown dashed.

4.11 Interference of two states

In section 4.10 we took a closer look at the interference in the cross section between different states. To investigate this further the S-matrix model (sec. 2.3) was used. The value $|1 - S|^2$, corresponding to the cross section, was studied as a function of the energy [16]. This value can not be larger than 4 due to the unitarity of the S-matrix. Two states with energy +0.1 and -0.1 were used. Both states are however unbound, because there are no thresholds in the model used. Additionaly, the corresponding Breit-Wigner shapes were calculated from the corresponding real and imaginary part of the eigenvalues of the effective hamiltonian.

For a small α^{ex} (0.08), well below the critical point, the energies of the states are not shifted and the widths are rather small. The states are well isolated. Nevertheless, the interference between the states gives rise to a visible difference between the Breit-Wigner shapes of the states and the calculated cross section.

At the critical point, $\alpha^{ex} = 1$, the two states lie at the same energy (0 MeV) and have the same widths. In the calculated cross section, however, an interference minimum exists at E=0. Naively one could interprete the calculated cross section as arising from two isolated states starting to interfere.

For a large α^{ex} (4), both states still have the same energy, but one state is broad and the other one narrow. The narrow state is visible as a dip in the structure of the large one.

Chapter 5

DISCUSSION OF THE RESULTS

5.1 Absence of threshold in the eigenvalue picture

In 4.5 it is shown that the shape of the eigenvalue picture is dependent on the energy of the system. The question for this section is what influence the shift of the closed system energies 'by hand' in our calculations could have.

We looked at the eigenvalues of the effective hamiltonian, $H^{eff}_{QQ} = H_{QQ} + H_{QP}G^{+}_{P}H_{PQ}$, and in the used representation H_{QQ} is diagonal with the shifted closed system energies E'_R minus the Q-value as elements. The $\tilde{\varepsilon}_R$ are the solutions of the matrix eigenvalue equation 2.33. It is always true that for a matrix M with eigenvalues E, i.e. $(M - E)X = 0$, $M \rightarrow M + cI$ implies $E \rightarrow E + c$.

To put this in other words for our case: When solving 2.33 with eigenvalues of H_{QQ} shifted to around the elastic threshold, we could always first add 1000 MeV to the shifted energies and then subtract 1000 MeV from $\tilde{E}_R$, thus being very far from the threshold when solving. Therefore the shift of the shell model energies and the actual position of the threshold can have no other influence whatsoever to the shape of the eigenvalue picture but the positon of zero of the energy axis. There can not be any thresholds in the eigenvalue picture calculated at a fixed energy of the system. States therefore can have negative resonance energy and a finite imaginary part of the effective eigenvalue (of course calculated at positive energy of the system). The problem is only how to interprete these values. We call states with negative resonance energy 'negative states' and states with positive resonance energy 'resonances'.

It should be noted that this discussion does not apply to the cross section, because it depends explicitly on the energy E_{lab} of the system and it can be calculated already from 2.30 without diagonalizing of H^{eff}_{QQ}. Furthermore, when solving the fix point equation 2.43 of course the actual position of zero of the energy axis is important.

From this discussion it follows that we do not have any reason to suspect any new phenomena in the eigenvalue picture close to the threshold. The trapping ought to be observable, and that is what the numerical results show, indeed.

Furthermore, by changing the border conditions the negative states could be studied directly. The reaction (d,p) corresponds to a neutron reaction with negative energy. Also, photon reactions could be considered. For negative energies of the system , the second term of H^{eff}_{QQ} (2.29), $QV^{res}P * G_P * PV^{res}Q$, can not have an imaginary part, but the real part still can mix the states and thereby giving a correction to the resonance energies $\tilde{E}_R$ and wavefunctions $\tilde{\Phi}_R$.

5.2 Effects at low energy of the system

We consider the shape of the eigenvalue picture for $E_{lab} = 4$MeV described in 4.6 and ignore the threshold.

The striking feature is the slope: smaller widths for states at larger resonance energies. This slope is much more pronounced at $E_{lab} = 4$ MeV than at 29 MeV. In section 4.9, the slope is understood as an effect of both the internal and the external mixing, both of which prefer states with lower resonance energies. The reason why the lower energies are prefered is that the nuclear force is attractive.

For the selected shift and Q-value the slope does imply that the 'broadest' states are negative states. For reasons that will be explained in chapter 6, we do call these states 'collective' states.

5.3 Cross sections

In 4.3 we would naively see a new effect: an ensemble at high level density without a broad state. This would contradict the earlier results concerning the slaving principle. However, from the eigenvalue picture 4.6a, we give a different interpretation: the 'broad' state was formed in the negative part of the spectrum.

From the figure 4.3 we learned that the negative states also directly can influence the cross section. A collective state that would have had a certain width and a certain energy if the energy shift was slightly smaller still can show its tail in the resonant part of the spectrum.

It should be noted that this kind of effect can be seen in the neutron scattering but is difficult to see in a cross section for proton scattering, because the Coulomb repulsion implies that the cross section has to go to zero as the lab energy goes to zero.

Finally, the two sections 4.10 and 4.11 give a strong warning when trying to identify states in a measured spectrum. The interference between the states can give rise to strange results.

5.4 Neutron Resonances

The result that the negative states can trap the resonant states is of special interest for the neutron resonances lying in the very neighbourhood of the elastic threshold. In the cross section for neutron scattering at heavy nuclei, a set of narrow resonances close to the elastic threshold can be seen. They have widths in the order of keV, or even eV, and spacings of the same order of magnitude. The states are well separated.

From our investigations a possible explanation for this phenomenon can be stated: It is possible that these resonances are trapped by a collective state. It is known that the wavefunctions of the neutron resonances are strongly mixed, which, in combination with the fact that they are close to the threshold, leads to their small widths. Strong mixing is a signature of trapping. Furthermore, single-particle resonances exist and are often discussed in order to explain the observed correlations between the neutron resonances [17]. They may correspond to our broad states.

As a conclusion of this chapter I show some measured total neutron cross sections close to the elastic threshold for uran from [19], fig. 5.1. We can see the typical energy scale eV or keV and the interference effects between states at high level density as discussed in section 4.10 and 4.11.

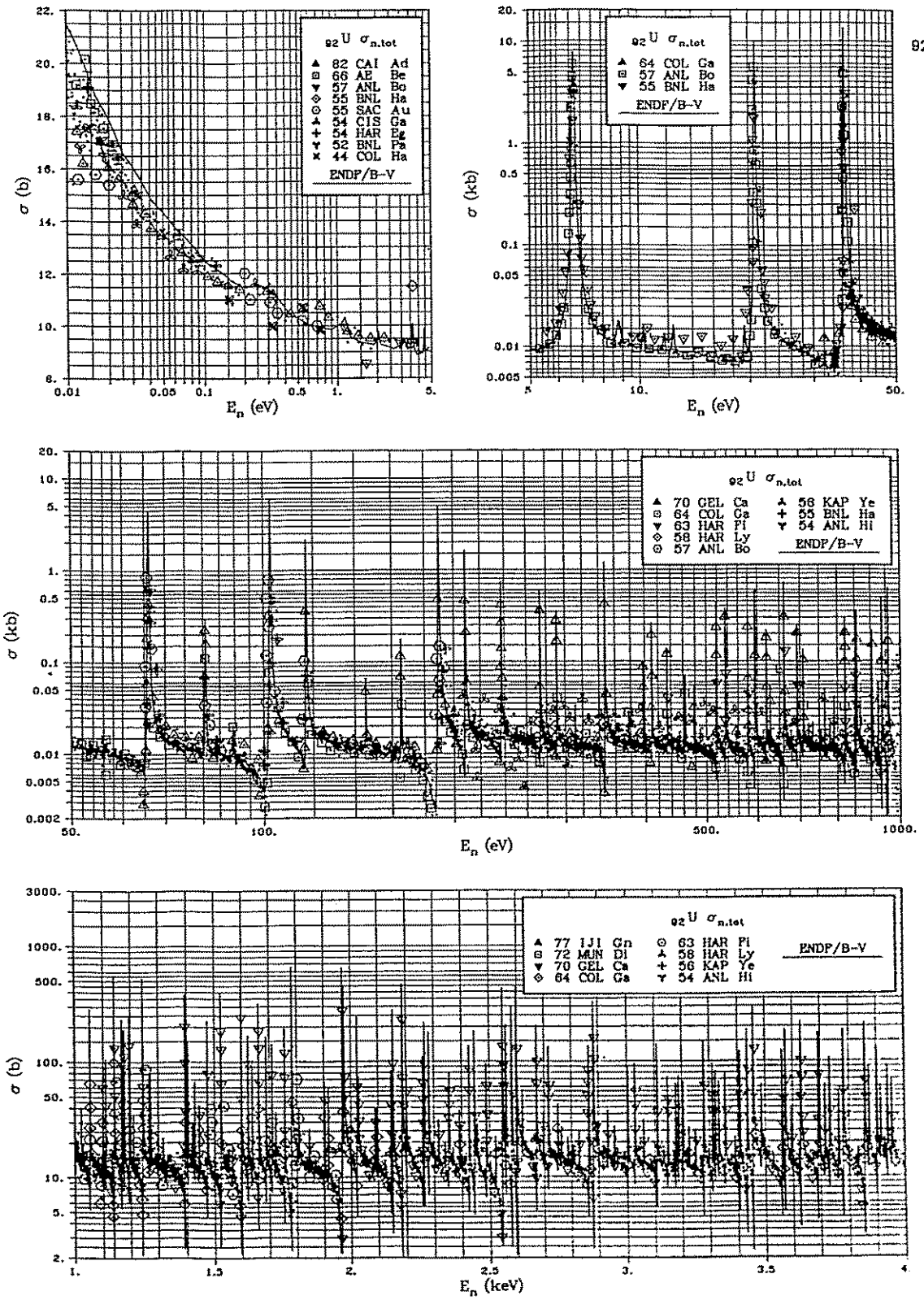

Figure 5.1: Measured neutron cross sections for uran from [19].

Chapter 6

NUCLEAR STRUCTURE OF STATES AT HIGH LEVEL DENSITY

As stated in 2.2.3 the solutions of the fixpoint equation 2.43 are considered to describe the width and energy positions of exited states in the compound nucleus. To consider an ensemble of states around the elastic threshold gives rise to some difficulties. When studying neutron scattering reactions, states below the elastic threshold can not be studied directly, because the kinetic energy of the neutrons is always positive. The negative states do not exist in these investigations, and they certainly do not have the possibility of decaying into a neutron channel. The fixpoint equation 2.43 can not be solved. The states could be investigated by using other reactions, but this chapter concerns the question how to interpret the complex eigenvalues of the effective hamiltonian 2.29 in the case neutron scattering.

The simplest interpretation is possible on the basis of the results given in chapter 4. As the negative states can trap the resonant states and also directly influence the cross section, we could loosely say that the combination of width and negative energy position of a negative state gives us a measure of how much that state could influence the positive energy area. Making such a statement however is very qualitatively. How broad a distant state has to be to be able to trap states is not quantitatively understood. Further, because of the interference effects between the states the influence of a certain state to the cross section is a complicated question. The aim of this chapter therefore is to try to understand what a large imaginary part of an eigenvalue of the effective hamiltonian means in a way that does not include the question of lifetimes or widths.

In 5.1 it was stated that when considering the complex eigenvalues at a certain energy E_{lab} of the system, the threshold can have no effect at all. Therefore, when an understanding of the complex eigenvalues can be found far from threshold, it must also hold close to threshold.

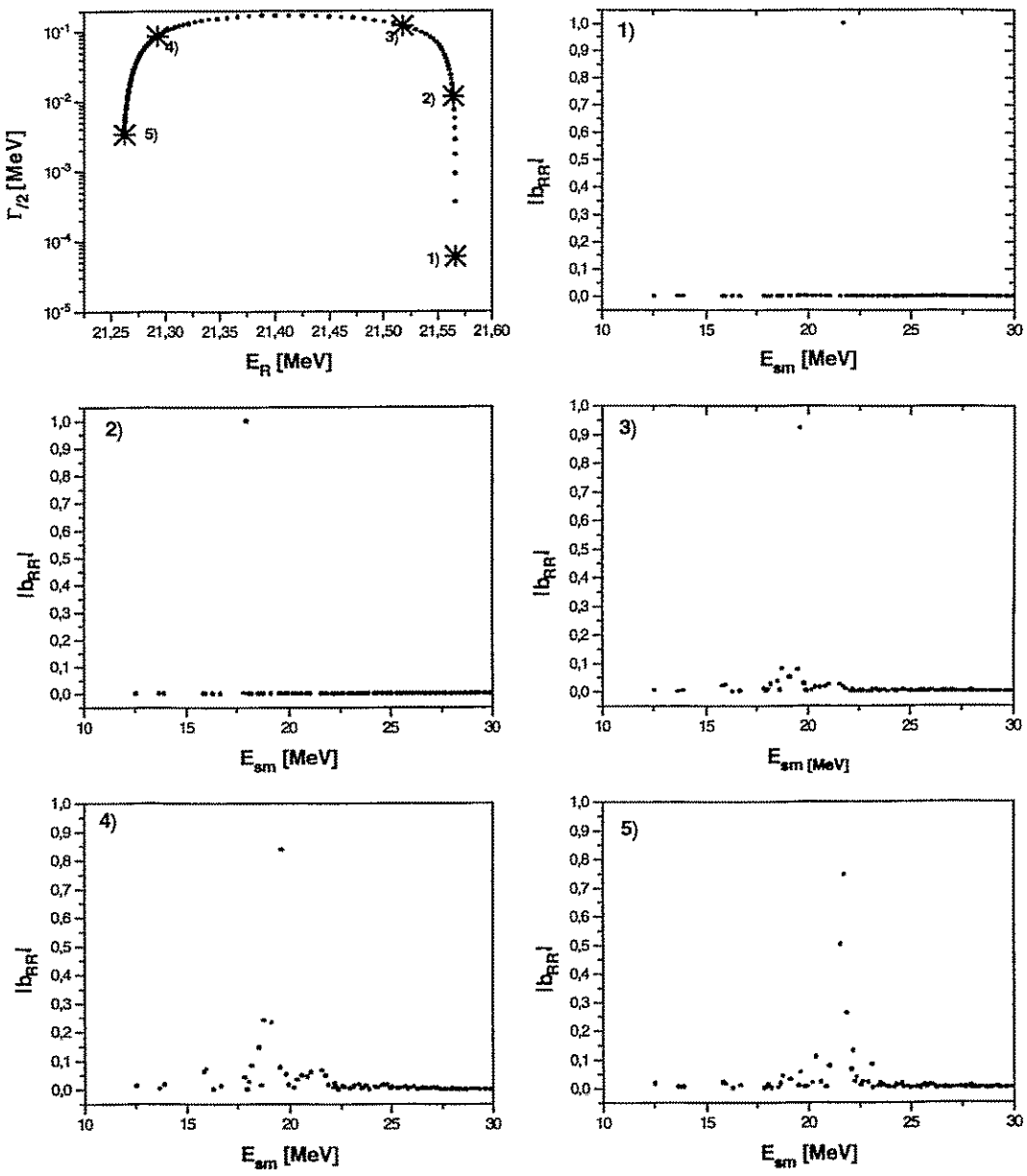

Figure 6.1: The absolute value of the expansion coefficients for one trapped QBSEC versus the shell model states for five different α^{ex}. $E_{lab} = 29$ MeV, $Q = 20.691$ MeV, $E^* = 6.149$ MeV, $E'_{sm} = E_{sm}$ and $\alpha^{ex} = 0.05, 0.5, 1.5, 3.0, 10$.

6.1 Distribution of the coefficient expansion

This section deals with the question to what extent any relation between the $\tilde{\Gamma}_R$ and the complex expansion coefficients $b_{RR'}$ of 2.36 can be established (fig. 6.1).

The situation for small α^{ex} almost exactly corresponds to the closed system. Thus, for a state R' with energy $\tilde{E}_{R'}$ and the state R with the corresponding energy, $b_{RR'}$ will be almost real and almost equal to one, and all the other coefficients will be almost zero.

As α^{ex} , and thereby $\tilde{\Gamma}_R$, grows, we can see a distribution in the plot of the absolute value of the coefficients versus the shell model energies. The width is centered around the state R and expires almost no shift that would correspond to the shift of $\tilde{E}_R$. The distribution has a width according to $\tilde{\Gamma}_R$.

For larger α^{ex}, when $\tilde{\Gamma}_R$ of the trapped states start to decrease, the inverse is not true however. The width of the distribution in the coefficient plot does not decrease with $\tilde{\Gamma}_R$.

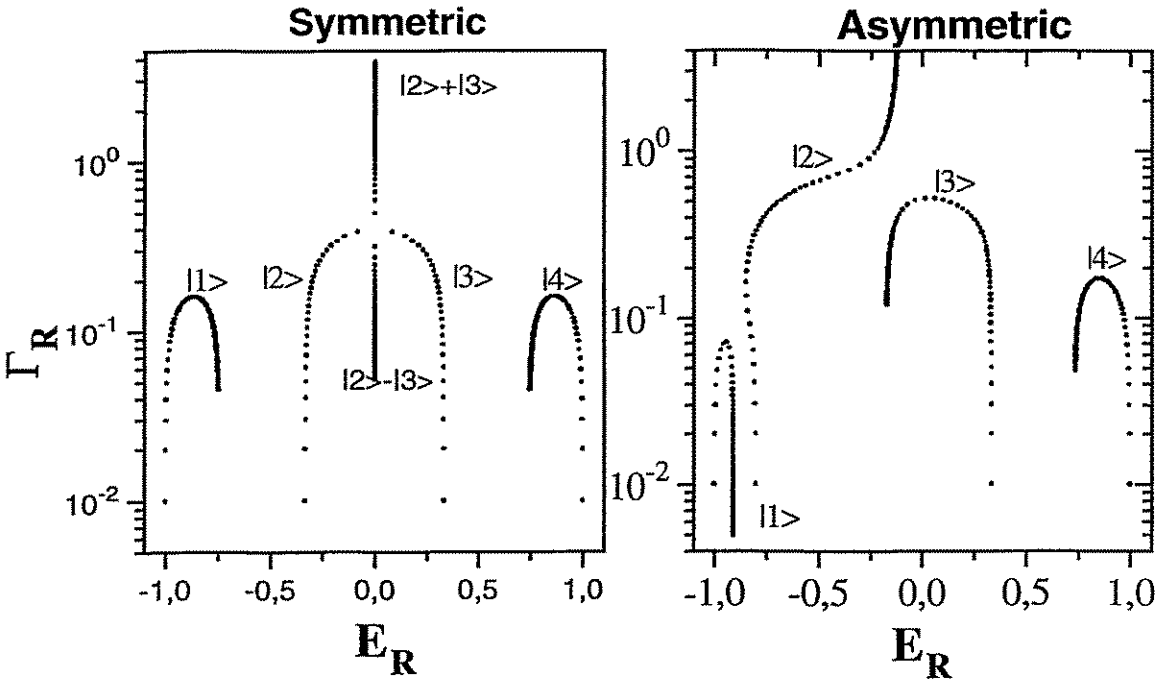

Figure 6.2: Eigenvalue picture in the S-matrix-model for α varied from 0.02 to 2 in steps of 0.02 for symmetric and asymmetric initial position of 4 resonances.

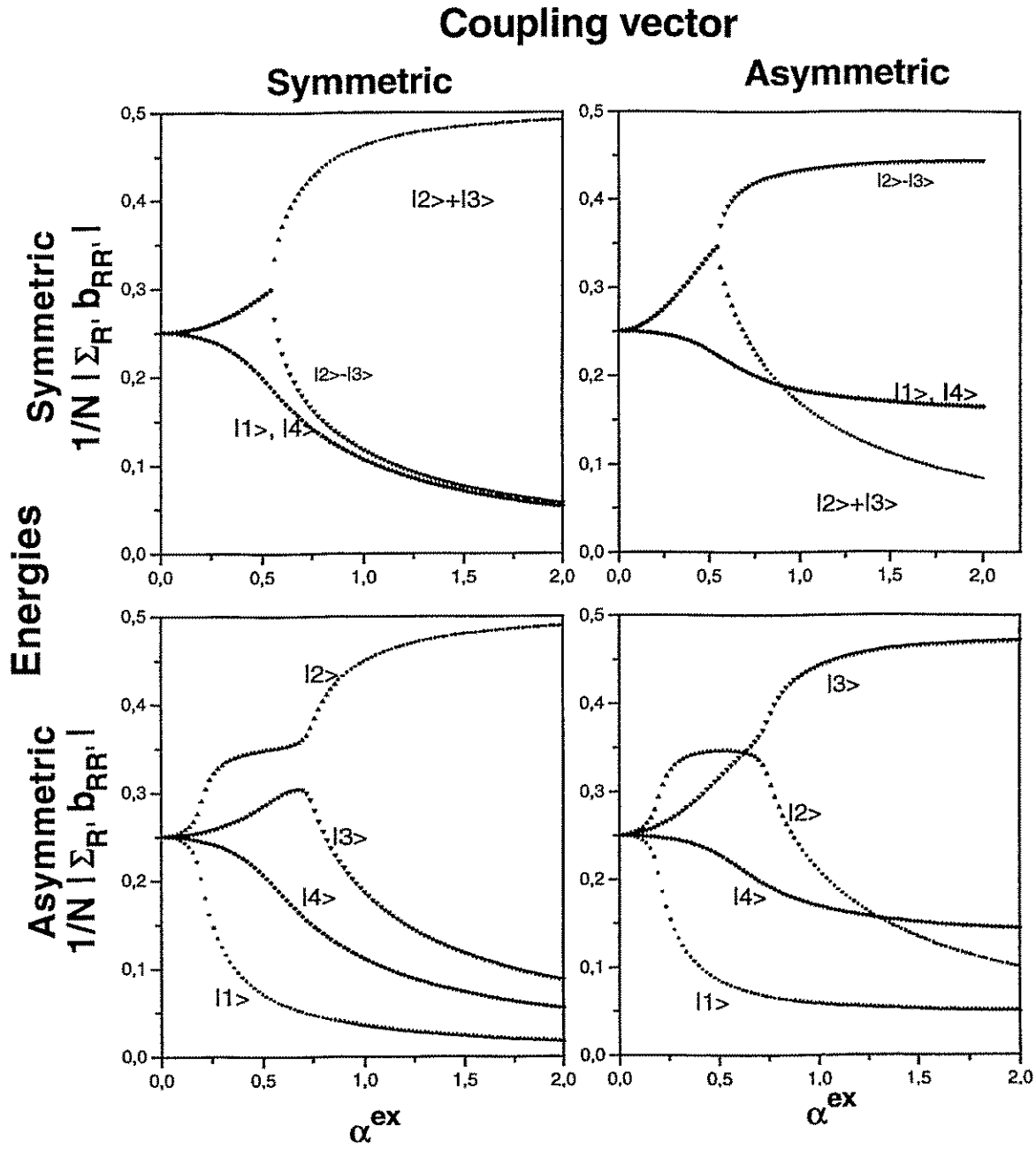

Figure 6.3: $\frac{1}{N} \mid \sum_{R'} b_{RR'} \mid$ versus α^{ex} for symmetric and asymmetric decay channel and selection of initial energies.

6.2 Rotation of the broad state

In the simple S-matrix model (described in 2.3) α^{ex} has been varied for four cases [16]. $V = \alpha^{ex} * V^0$. In all cases four states were used, one channel was open and α^{ex} varied from 0.02 to 2 in steps of 0.02. H^0 was chosen symmetric(-1,-1.33,1.33,1) or asymmetric (-1, -0.8, 1.33, 1). The vector V^0, describing the coupling to the decay channel was chosen (0.5, 0.5, 0.5, 0.5), i.e. symmetric, or antisymmetric, (0.5, -0.5, 0.5 ,-0.5).

The eigenvalues are shown for symmetric and asymmetric initial position of the energies of the states in fig. 6.2. The eigenvalues do not distinguish between symmetric and asymmetric channel channel. In 6.3 the average of the coefficients $\frac{1}{N} \mid \sum_{R'} b_{RR'} \mid$ versus α^{ex} is shown for the four states in the four cases.

The interesting fact is that for the two cases with symmetric coupling vector, the sum $\frac{1}{N} \mid \sum_{R'} b_{RR'} \mid$ for the broadest state has the largest value. In the asymmetric cases it has smaller values. Of special interest is the asymmetric-asymmetric case. The broadest state has the largest value for the average of the coefficients only at small α^{ex}. As α^{ex} approaches the critical point ($\alpha^{ex} = 1$) we can clearly see that the average starts to decrease and for $\alpha^{ex} = 2$ the broad state has the second smallest average.

The interpretation of this section is as follows: For small α^{ex} the state vectors point into the direction of the closed system (one coefficient equals 1 and the rest 0, i.e. the sum is 0.25). As α^{ex} increases, the states start to rotate.. The state that will achieve a short lifetime, must rotate into the direction of the decay channel. The corresponding average for the coupling vector describing the decay channel is 0.5 for the symmetric case and 0 for the asymmetric case.

6.3 Discussion

For small α^{ex}, the state vectors point in the hilbert space in the direction of the states of the corresponding closed system. When $\tilde{\Gamma}_R$ grow, the states rotate into the direction of the decay channel. When the $\tilde{\Gamma}_R$ of the trapped states start to decrease must the vectors of the trapped states rotate in an arbitrary direction away from the structure of the decay channel, but not necessarily in the direction of the corresponding closed system vector.

All these results are qualitatively understandable: The width corresponds to the inverse lifetime, and the lifetime is governed by the degree of overlap between state and decay channel.

The point is that these statements should be true for both the resonant states and the negative states. Thus, the widths $\tilde{\Gamma}_R$ at $E_{lab} \geq 0$ for the negative states are an expression for their nuclear structure in the same manner as they characterize the nuclear structure in the case of the resonant states. This is the reason why we call the negative states with large $\tilde{\Gamma}_R$ collective states.

Chapter 7

SUMMARY

In this work, the influence of a particle decay threshold on the redistribution taking place in the nuclear system under the critical condition of high level density was investigated.

It is numerically and analytically shown that the trapping effect investigated in the system far from threshold by Rotter and co-workers also must work over the threshold for neutron scattering. Negative nuclear states, that would be resonances if the Q-value was smaller, can trap the resonances. It is also numerically shown, that the broad state is preferably formed in the low-energy part of an ensemble close to the elastic threshold. Therefore an ensemble with energies around the threshold and the 'broad' state lying in the negative part of the spectrum may exist (such a state is called collective). In this case, the states with positive energies, which could be investigated with neutron scattering experiments, are all trapped. This could give a theoretical explanation for the results of neutron scattering at energies close to the elastic threshold in heavy nuclei.

Furthermore, the neutron scattering cross section for the case when the collective state has an energy only slightly below the elastic threshold was calculated. The tail of the collective state can be seen directly as a difference between the direct part and the total cross section.

The calculations up to now are made for one particle scattering on ^{15}O and ^{15}N only, and high level density is simulated by giving the parameter α^{ex} a non-realistic high value. For heavy nuclei, the natural level density is much higher. Thus for being able to perform a realistic comparison between experimental data and theoretical calculations for neutron scattering, calculations must be performed for heavy nuclei.

Generally, it makes no sense to speak about the width of a state with negative energy. In order to find another interpretation of the imaginary part of the complex eigenvalues of the effective hamiltonian (calculated at positive energy of the system), the expansion coefficients of the states coupled to the continuum versus the closed system states are investigated. It is shown that the structure of the broad state is similar to the structure of the decay channel. This is also true for the negative states.

The collective structure of the broad state is a result of the redistribution taking place at a critical value of the coupling to the continuum. The structure shows the important role which the environment of decay channels plays in this process.

Bibliography

[1] I. Prigogine, *From Beeing to Becoming - Time and Complexity in Physical Sciences.* W. H. Freeman and Company, San Francisco.

[2] Haken, *Synergetics* and *Advanced Synergetics.* Springer-Verlag, Berlin.

[3] Haken, *Information and Selforganization* Springer-Verlag, Berlin.

[4] P. Kleinwächter and I. Rotter, *Spectroscopic Properties of Highly Exited States.* Phys. Rev. C **32** 1742 (1985)

[5] I. Rotter *A continuum shell model for the open quantum mechanical nuclear system.* Rep. Prog. Phys. **54** (1991), 632-682

[6] W. Iskra, M.Müller, I. Rotter *Selforganization in the nuclear system, I: The slaving principle.* J.Phys.G: Nucl. Part. Phys. **19** (1993), 2045-2062.

[7] W. Iskra, M. Müller, I. Rotter *Selforganization in the nuclear system, II: Formation of a new order.* J.Phys.G: Nucl. Part. Phys. **20** (1994), 775-786.

[8] W. Iskra, M. Müller and I. Rotter, *Radial Pattern of Nuclear Decay Processes.* Phys. Rev. C (1995) (in press)

[9] R. U. Haq, A. Pandey and O. Bohigas, *Fluctuation Properties of Nuclear-Energy Levels - do Theory and experimental Agree.* Phys. Rev. Lett. **48** 1086 (1982)

[10] F. M. Dittes, I. Rotter and T. H. Seligman, *Chaotic Behaviour of Scattering Induced by Strong External Coupling.* Phys. Lett. A **158** 14 (1991)

[11] W. Iskra, I. Rotter and F. M. Dittes, *Hierarchical Trapping of Resonance States at High Level Density.* Phys. Rev. C **47** 1086 (1993)

[12] V. V. Sokolov and V. G. Zelevinsky, *On a Statistical Theory of Overlapping Resonances.*

Phys. Lett. B **202** 10 (1988)

[13] V. V. Sokolov and V. G. Zelevinsky, *Dynamics and Statistics of Unstable Quantum states.*

Nucl. Phys. A **504** 562 (1989)

[14] F.-M. Dittes, W. Cassing, I. Rotter, *Avoided resonance overlapping in many-channel scattering.*

Z. Phys. A 337, 243-245(1990)

[15] I Rotter, *External mixing of resonance states.*

J. Phys. G: Nucl. Phys. Vol. 5, No. 2, 1979.

[16] M. Müller, *Zur Herausbildung verschiedener Zeitskalen beim Zerfall von Compoundkern Resonanzen als Folge des Trapping-Effects.*

FZR-79 (Preprint Rossendorf march 1995).

[17] A. Bohr and B Mottelson, *Nuclear Structure, vol 1.*

Benjamin, New York, 1969.

[18] C. Mahaux and H. A. Weidenmüller, *Shell Model Aproach to Nuclear Reactions.*

Amsterdam: North Holland, 1969

[19] *Neutron Cross section.*

S. F. Mughabghab, M Divadeenam and N. E. holden,

Volume 1: Neutron Resonance Parameters and Thermal Cross Section.

V. Mc Lane, C. L. Dunford and P. F. Rose,

Volume 2: Neutron Cross Section Curves.

Academic Press Inc. (London) L.T.D. (1988)

ACKNOWLEDGEMENTS

First of all I would like to thank my supervisor at the Institute of Nuclear and Hadronic Physics of the Research Center Rossendorf near Dresden, Germany, Prof. Dr. Ingrid Rotter. When I made the descision that I wanted to do my master work in the field self *organizing systems I did not know how to be able to do that.* I learned about Prof. Rotter and her work and got into contact with her. She kindly invited me to do my master work in Rossendorf, for wich I am very grateful. I owe Prof. Rotter a most interesting year, both concerning my work at Rossendorf and the rest of my life there. I am also very thankful for stimulating discussions and good supervising.

I also like to thank Prof. Christoph Bargholtz at the Nuclear Physics Department of the University of Stockholm. He helped me to learn about Prof. Rotter and her work and kindly helped me to get into contact with her. Prof. Bargholtz also thereafter always supported me in all the practical things that needed to be arranged for this year.

I am also thankful to my supervisor at the University of Stockholm, Dr. Doc. Kjell Fransson, for all the support he has given me concerning this year in Dresden.

For good working conditions, I do owe thanks to the Research Centre Rossendorf and especially to the Director of the Institute of Nuclear and Hadronic Physics, Dr. Harald Prade.

I owe a special thank to Markus Müller, for all the help he has given me in learning about the subject of the research of the group at Rossendorf and in doing my master work.

Finally I would like to thank the other co-workers in the group in Rossendorf, Dr. W. Iskra, Dr. Frank Dittes and Thomas Gorin, for kindly helping me in doing my master work.